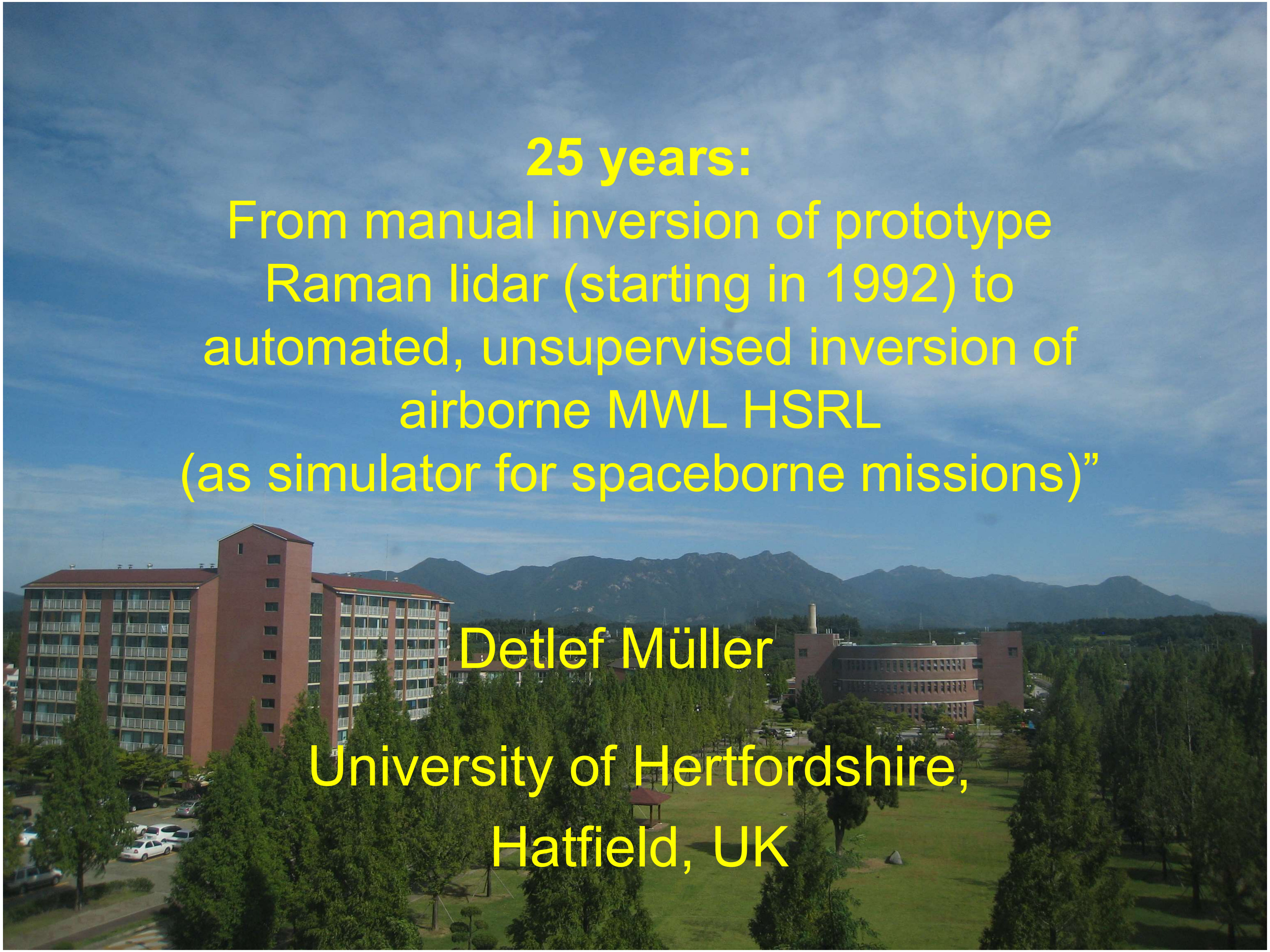

25 years:

From manual inversion of prototype Raman lidar (starting in 1992) to automated, unsupervised inversion of airborne MWL HSRL (as simulator for spaceborne missions)”

Detlef Müller

University of Hertfordshire, Hatfield, UK

OUTLINE

- **Motivation: Why Vertically Resolved Particle Properties (Optics, Microphysics, Chemistry)**
- **The Basis for the Retrieval of Microphysical Properties: Raman Lidar and High-Spectral Resolution Lidar**
- **Inversion Algorithm (start in 1994): Some Basics**
- **1998 – 2012: Examples of Results (Manual, Slow, Few)**
- **Since 2012: Examples of Results (Automated, Fast, Plenty)**
- **Outlook: Beyond: 2017**

The Effect of Aerosol Particles on Climate

Interaction of Radiation (Sun Light) with Particles

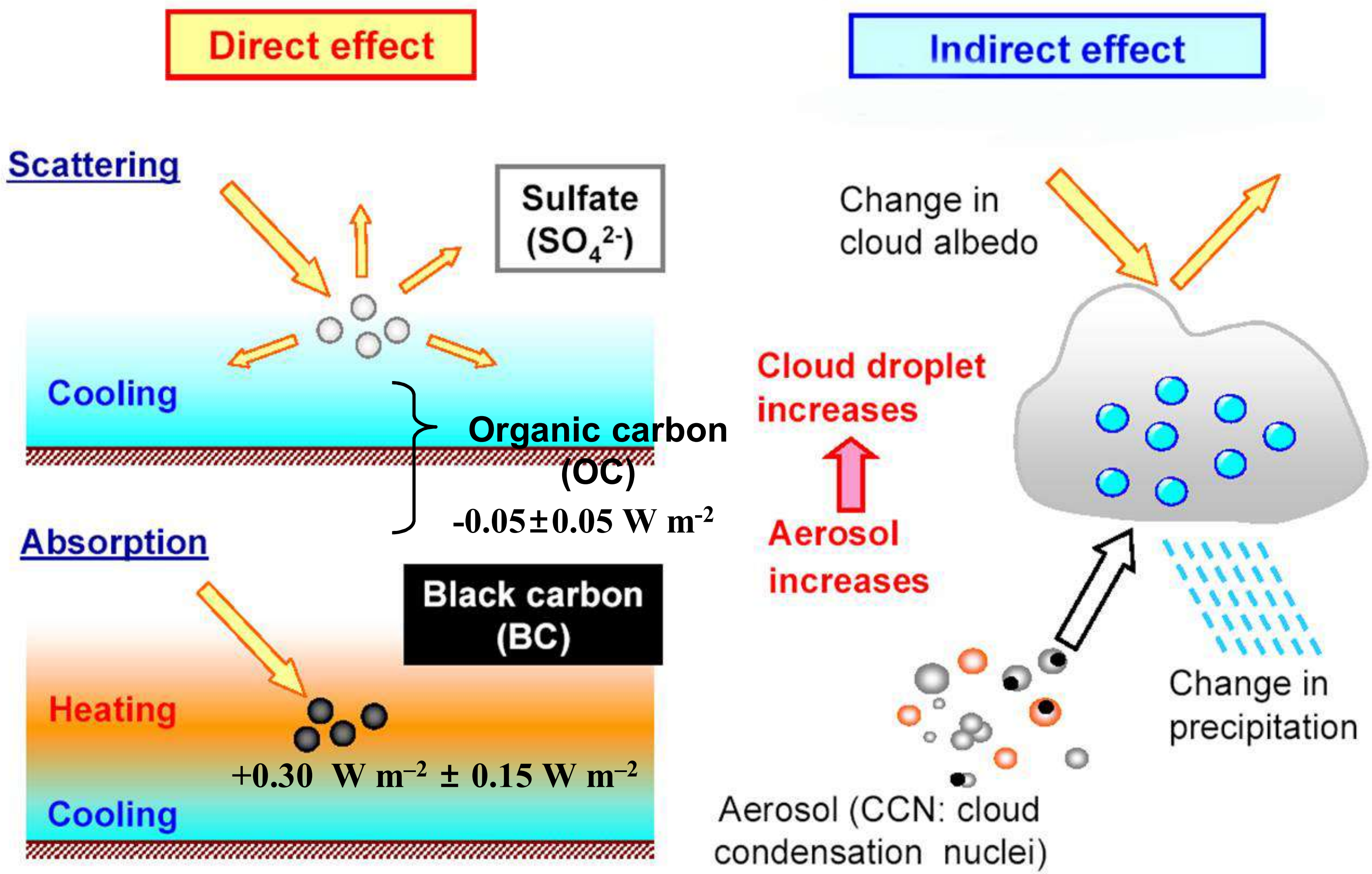

Importance of vertical position of particles

- Inluence on radiative transport (Quijano et al., JGR 2000):
  - “vertical position” of particle layers

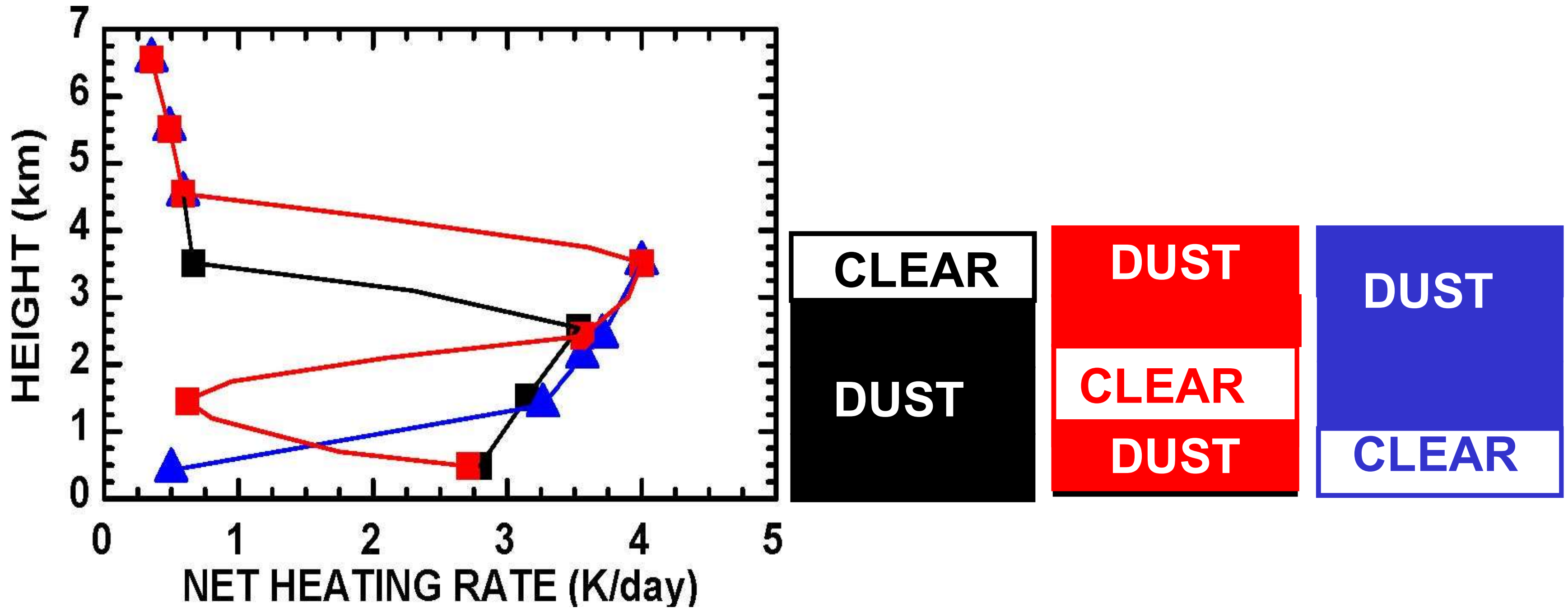

Vertically-Resolved Information on Particles

- **optical depth/extinction of aerosol particle layers**
- **single-scattering albedo and light-absorption properties**
- particle size distribution (mean particle size)
- refractive index
- particle shape
- **particle phase function**
- all these properties determine various aerosol types
  → desert dust, industrial pollution, forest-fire smoke, etc.

Mt. Pinatubo Eruption 1990: First Raman Lidar Observations of Particles

Ansmann et al.: Extinction and backscatter coefficient and lidar ratio in cirrus, PBL, and stratospheric aerosol (Mt. Pinatubo volcanic eruption) at nighttime and in PBL at daytime

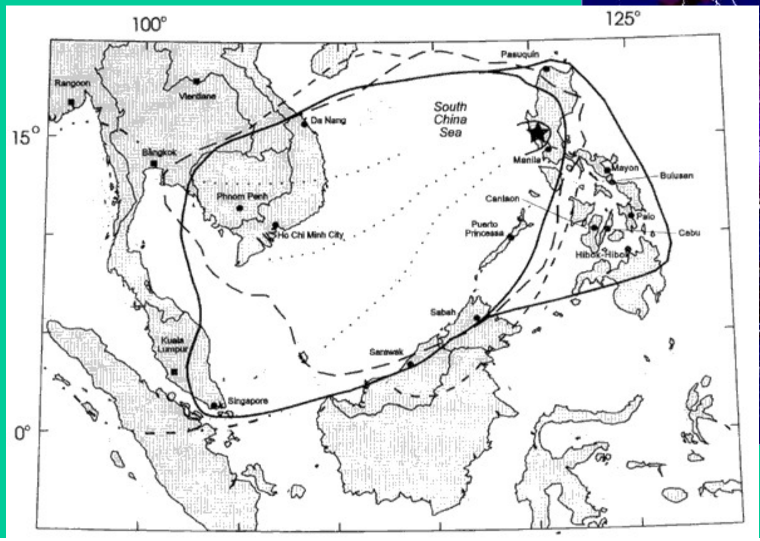

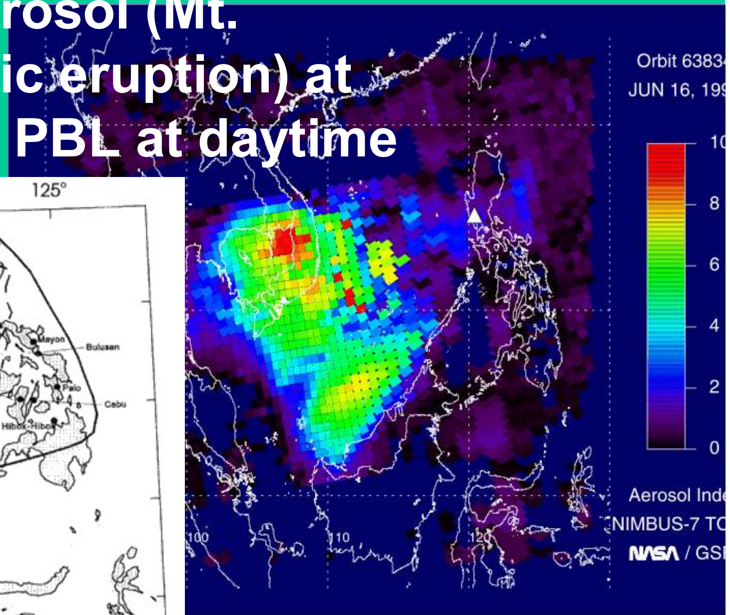

Parameters measured with Raman lidar

- Particle backscatter coefficient, $\beta(\lambda)$, **extensive**
  - Backscattering of radiation at 180° at wavelength (λ)

- Particle extinction coefficient, $\alpha(\lambda)$, **extensive**
  - scattering ($\sigma(\lambda)$) + absorption of radiation

- Particle lidar ratio, **$S(\lambda)$, intensive**
  - Extinction-to-backscatter ratio,

    $S(\lambda) = \alpha(\lambda)/\beta(\lambda)$ (same λ!!!)

- Particle depolarization ratio, $\delta(\lambda)$, **intensive**
  - for linearly polarized radiation: $\delta(\lambda) = \beta_{\perp}(\lambda)/\beta_{||}(\lambda)$

With $\perp$ denoting the cross-polarized component, and || denoting the linear-polarized component of radaitions, with respect to the transmitted radiation

Data Products Raman Lidar

Aerosol-typing based on optical properties

↑

- Lidar ratios:
  - qualitative information on size and refractive index > absorption
- Depolarization ratio:
  - shape

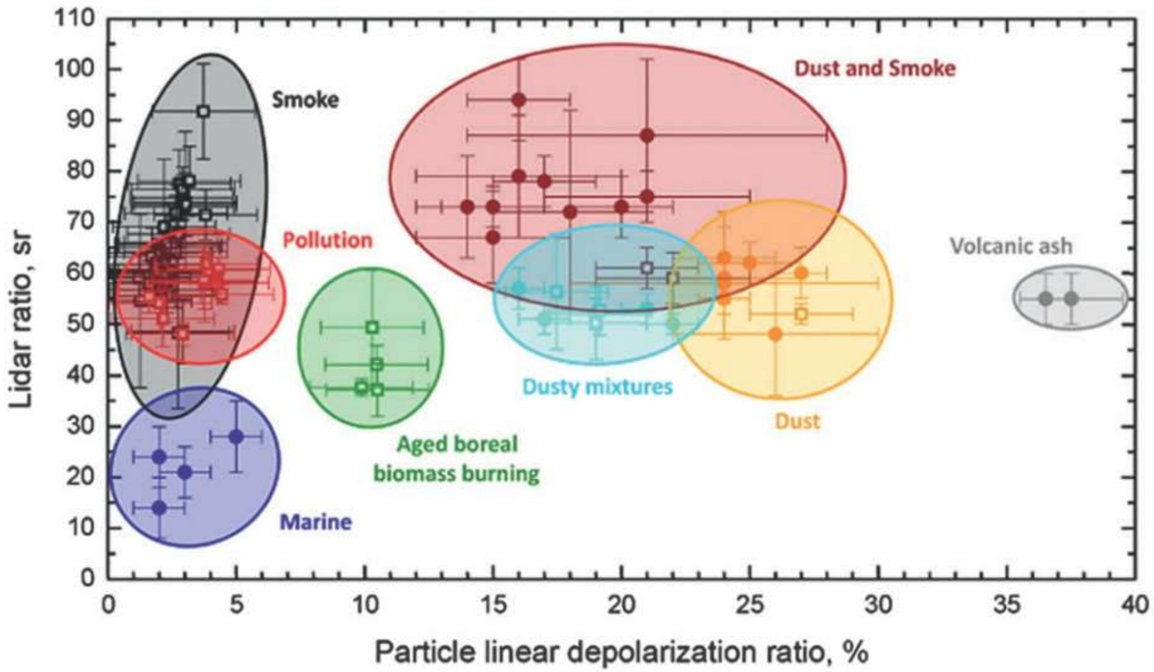

FIG. 8. Aerosol classification from measurements of lidar ratio and particle linear depolarization ratio at 355 nm. Ground-based observations were performed with the Raman-polarization lidars (POLIS) (University of Munich, dots) and Polly^{XT} (Leibniz Institute for Tropospheric Research, open squares) at Cape Verde (dust, marine, dust and smoke, dusty mixtures; dots; Groß et al. 2011); Leipzig, Germany (pollution, aged boreal biomass-burning aerosol, dusty mixtures; open squares); Munich, Germany (volcanic ash; dots; Groß et al. 2012); in the Amazon basin (smoke; open squares; Baars et al. 2012); and over the North Atlantic (dust, dust and smoke; open squares; Kanitz et al. 2013).

Multiwavelength Raman Lidar: 6β+2α+1δ prototype operational since 1996

-Backscatter coefficient

355, 400, 532, 710, 800, 1064 nm

-Extinction coefficient

355, 532 nm

-Water vapor

-Temperature

-Depolarization ratio

2nd Multiwavelength Raman Lidar: 3β+2α+1δ prototype operational since 1997

If we use multiwavelength lidar, we also measure:

- Ångström Exponent, å
  - $å = [\ln(\alpha(\lambda_1)) - \ln(\alpha(\lambda_2))] / [\ln(\lambda_2) - \ln(\lambda_1)]$

- Ratios of these parameters
  - e.g. Ångström exponent of the lidar ratio

Instead of Ångström exponent we can use color ratio

Information Content of Multiwavelength Raman Lidar

1) **Extinction-related Ångström exponents**
   → Particle size, (refractive index, RFI: chemical composition)
2) **Backscatter-related Ångström exponents**
   → Particle size, particle shape, RFI
3) **Extinction-to-backscatter (lidar ratio) ratio**
   → Particle size, RFI, particle light-absorption, particle shape
4) **Linear particle depolarization ratio**
   → Particle shape

- Aerosol types: qualitative description of aerosol properties
- Allows for identification of basic aerosol types
- More wavelengths at which a lidar operates means a better differentiation among aerosol types (mixing states!!!)

Classification of different aerosol types

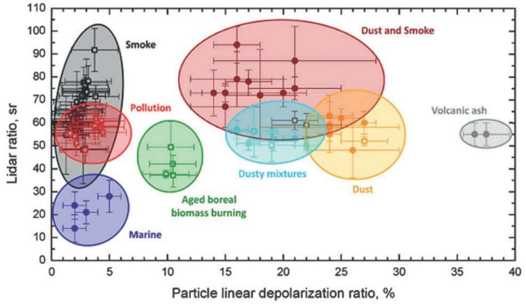

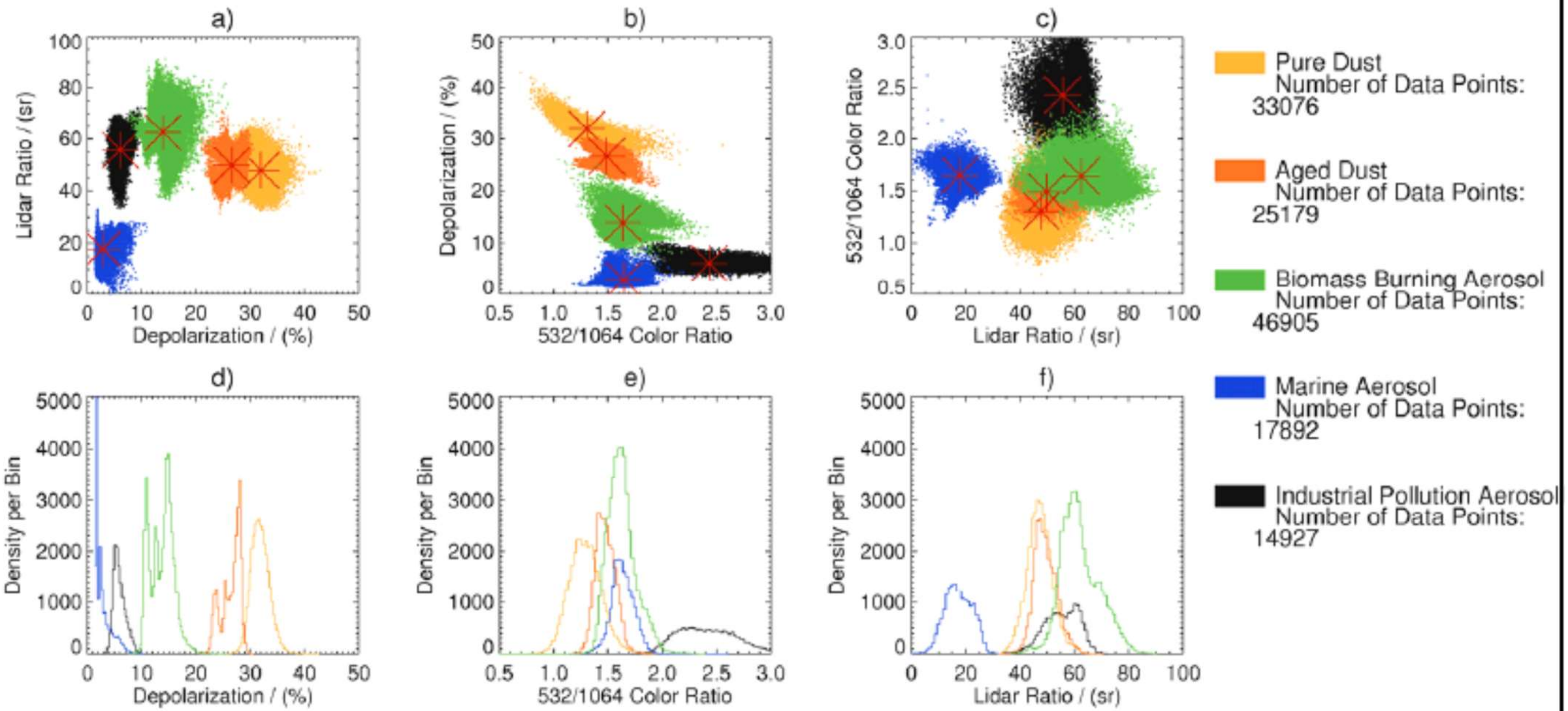

1064 nm channel corrected with constant S_a = 40 sr (-> induce uncertainties)
-> a further HSRL wavelength would allow for more accurate characterization

from: M. Esselborn, A. Petzold. et al., DLR, Germany

Aerosol typing: „finger print“

multi-wavelength, extinction, backscatter and depolarization lidar

→ aerosol-type classification from intensive optical parameters

- lidar ratios (355, 532 nm)
- color ratios/Ångström exponents (extinction and backscatter)
- particle depolarization ratio
- „ratio of ratios“

→ microphysical properties:

- depends on the *spectral* information „$3\beta+2\alpha$“ (backscatter at 355, 532, 1064 nm, extinction at 355, 532 nm)
- depolarization information important for particle shape (Mie-theory scatterers or non-spherical scatterers)

Data Inversion Technique, since 1997

Müller et al., Appl. Opt., 1998, 1999,2000

Particle Size Distribtion

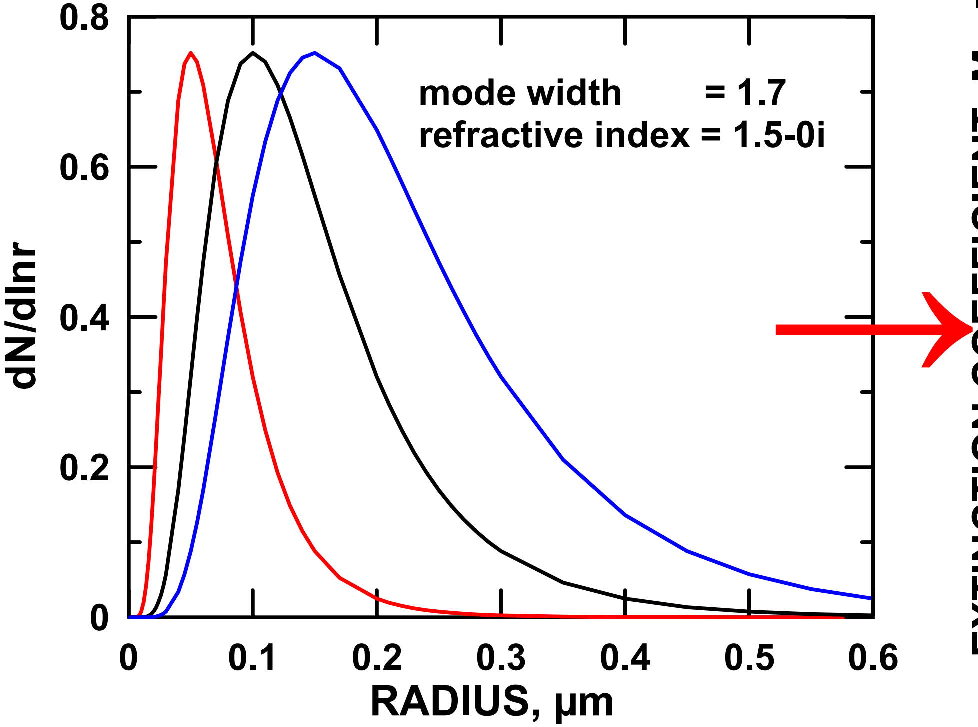

Angström-Exponent

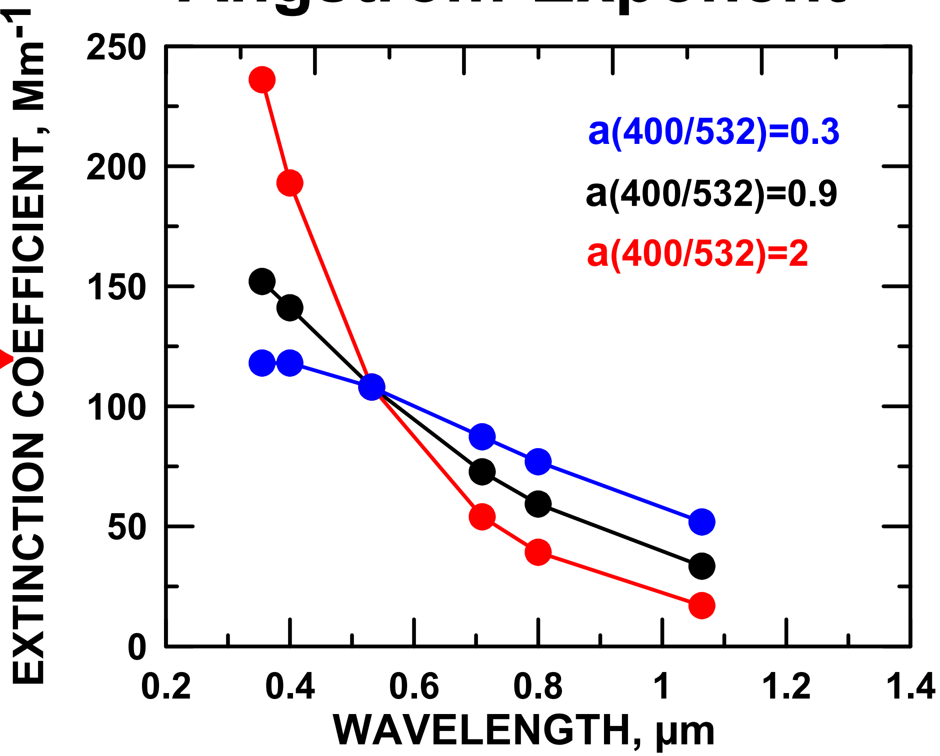

Lidar ratio

$$S = \frac{\alpha}{\beta} = \frac{\alpha_{str} + \alpha_{abs}}{\beta}$$

S = ~20→ sr marine particles

S = ~80 sr strongly absorbing particles

„Backward Calculation“

DATA INVERSION

infer size distribution refractive index from optical data

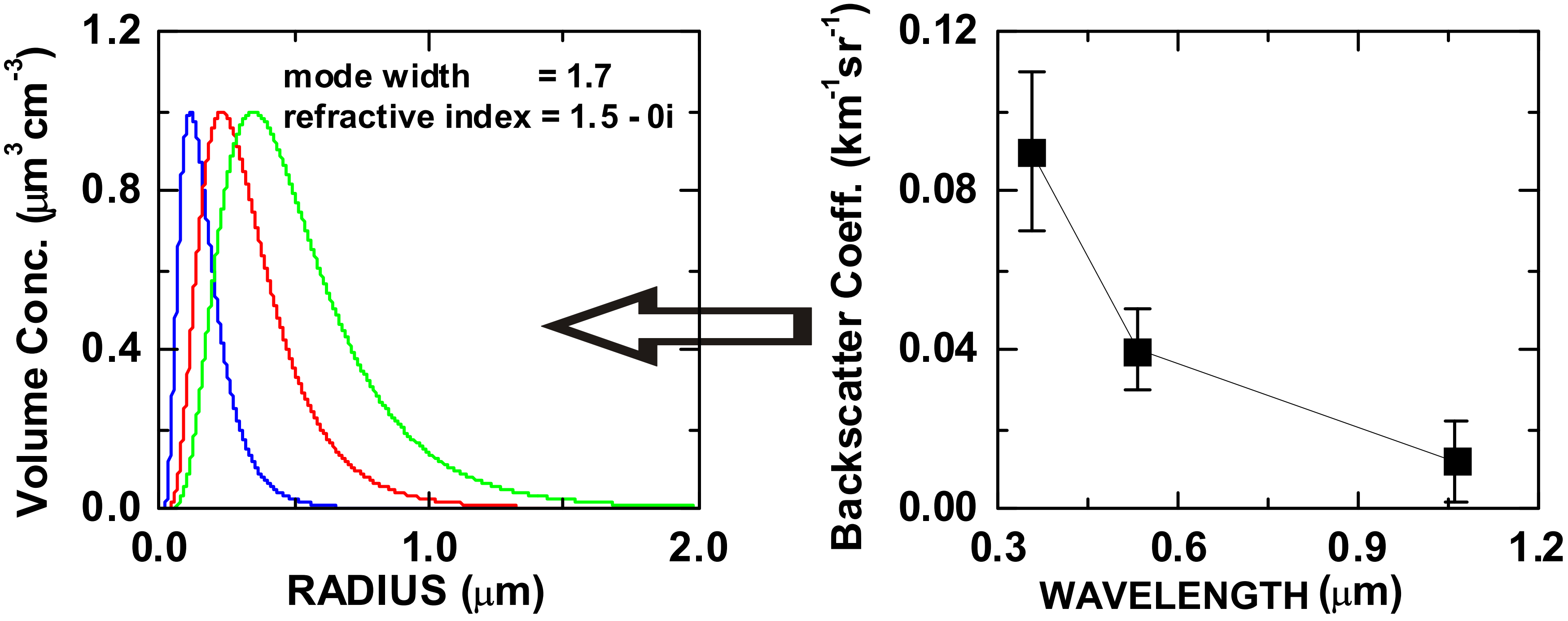

Microphysical Parameters
I only talk about to „3+2“ systems

We take all β(λ) and all α(λ)

↓

Inversion algorithm

↓

- mean (effective) radius
- Number, surface-area, volume conc.
- complex refractive index (real, imaginary)

→ single-scattering albedo: scat/ext
→ absorption coefficient
→ phase function

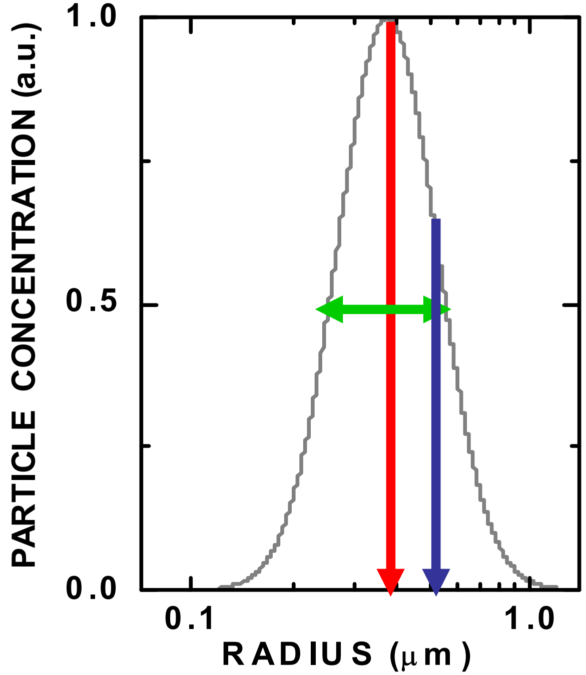

First we select data in height layers

Lidar measurement of profiles at several wavelengths

Spectrum of the backscatter coefficients and extinction coefficients

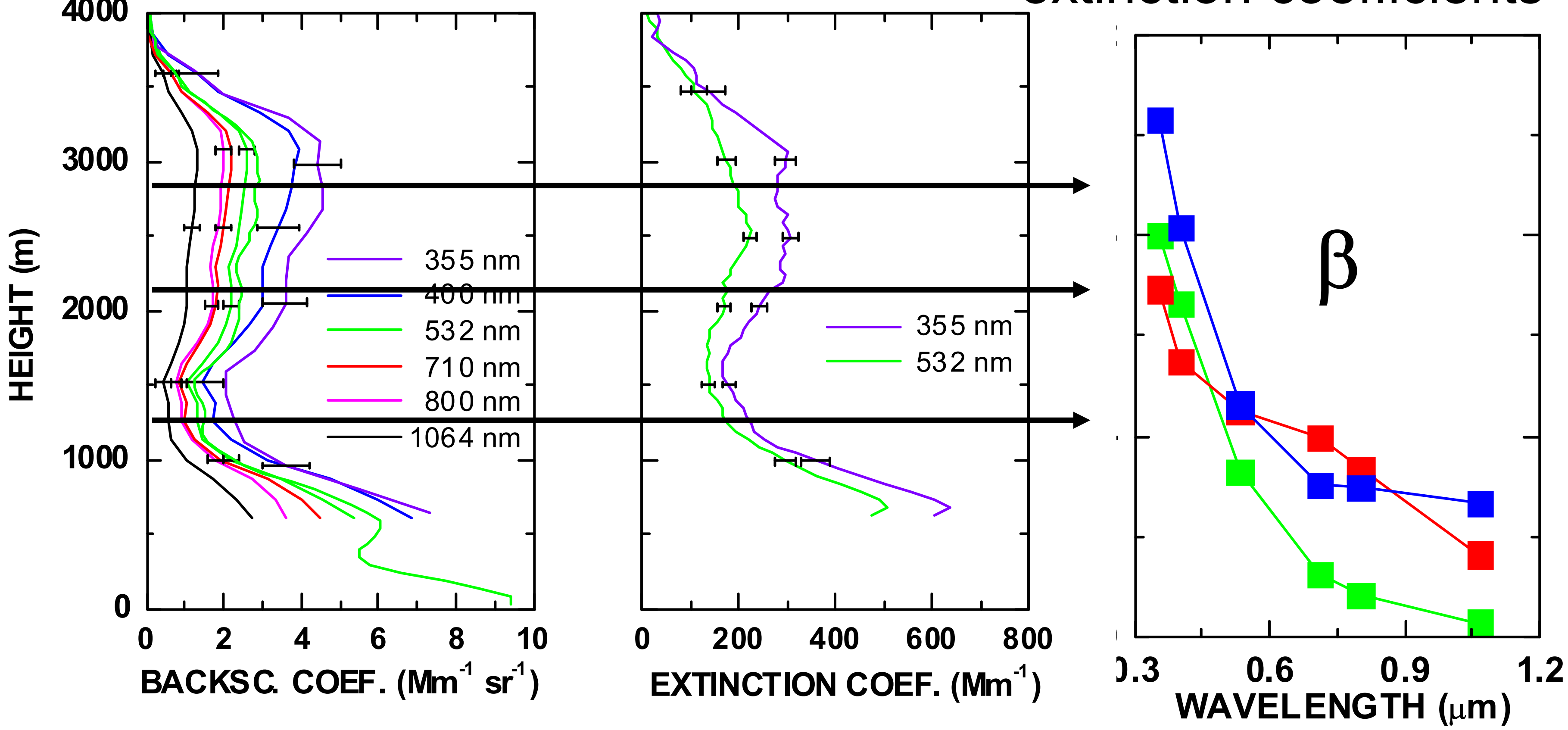

Fredholm Integral Equations of the First Kind

$$\overbrace{\beta(\lambda)}^{\text{Optical Data}} = \int_0^\infty \overbrace{K_\beta(r,m,\lambda,s)}^{\text{Kernel Functions}}\ \overbrace{v(r)}^{\text{Particle Size Distribution}}\, dr$$

$$\alpha(\lambda) = \int_0^\infty K_\alpha(r,m,\lambda,s)\ v(r)\, dr$$

Backscatter- and Extinctions Coefficients

Particle size

Complex Refractive Index

Wavelength

„Shape Property“

Volume Size Distribution

THE INVERSE PROBLEM

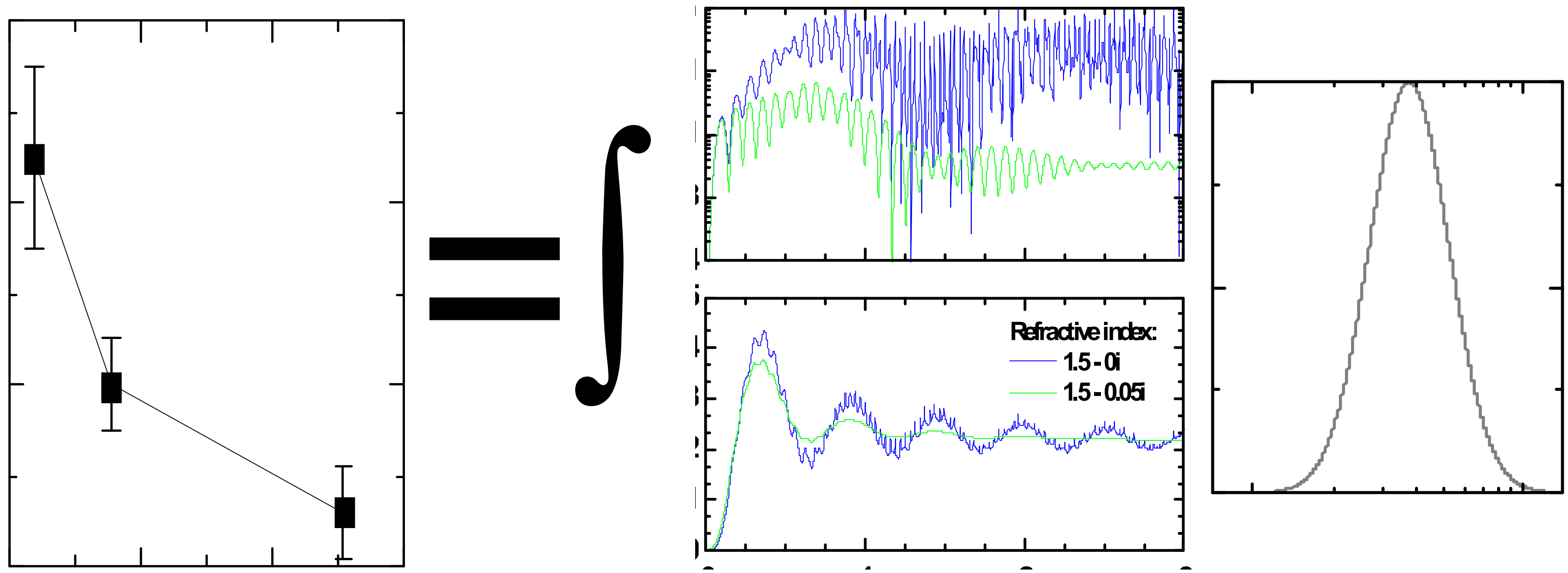

y = K x

The „idea“: We reconstruct the particle size distribution with „base functions“

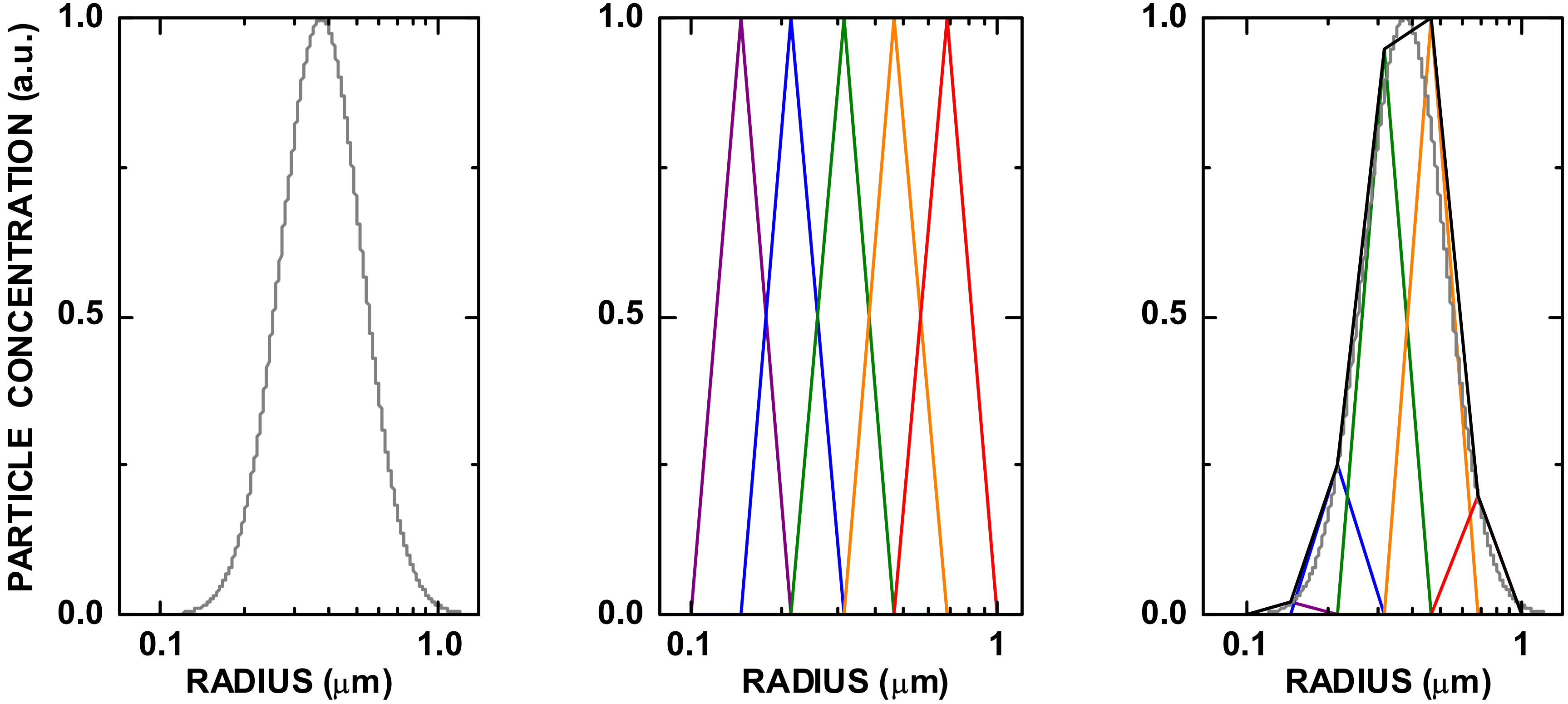

$v(r)$ $\qquad$ $B_j(r)$ $\qquad$ $v(r) = w_j\, B_j(r)$

The weight factors (w_j) are calculated in the inversion

NUMERICAL SOLUTION OF

$$\alpha(\lambda) = \int_{r_{min}}^{r_{max}} K_{\alpha}(r, m, \lambda, s)\, v(r)\, dr$$

$$\beta(\lambda) = \int_{r_{min}}^{r_{max}} K_{\beta}(r, m, \lambda, s)\, v(r)\, dr$$

$$\Downarrow$$

$$g = A\,w + \varepsilon'$$

$$\Downarrow$$

$$\| A w - g \| = 0$$

error from approximation with base functions, etc.

Kernel Matrix

Weight Factors

Optical Data

Unfortunately it is not that simple

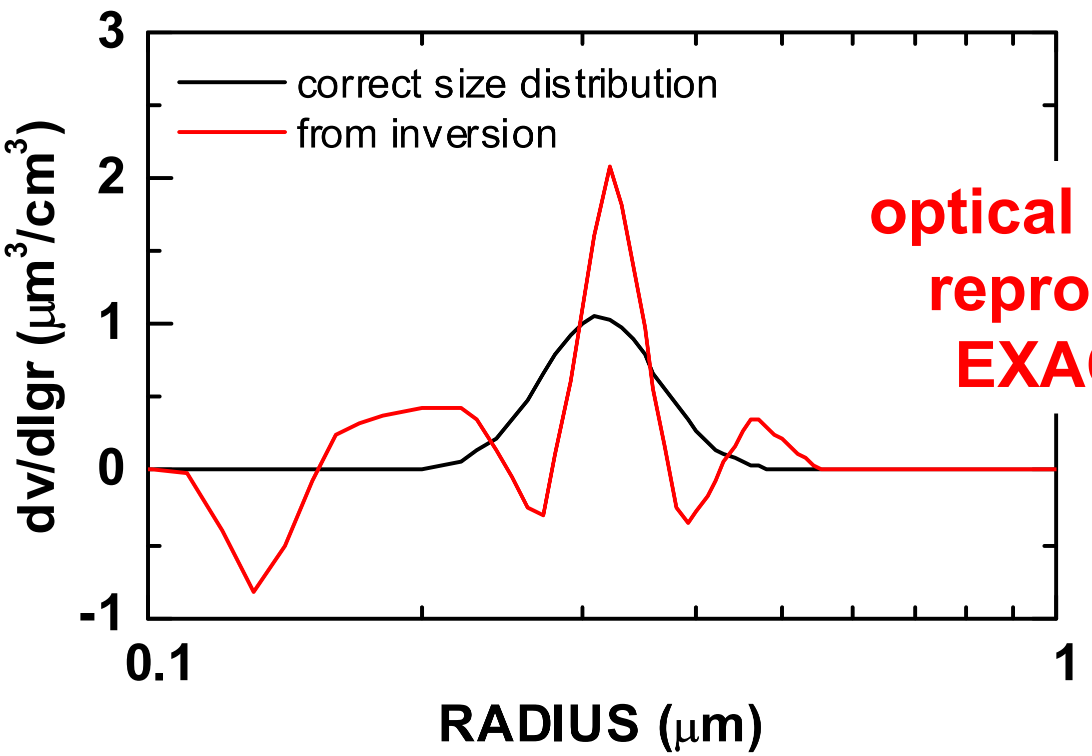

optical data are reproduced EXACTLY

Oscillations, or artificial modes, are typical for the inversion of lidar data

ILL-Posed Inversion Problems

- solution space is incomplete
- there are mulitple solutions (microphysics) for one optical data set
- Small errors (optical data) lead to large errors of microphysics

Regularization
turns ill-posed into well-posed problem

… is done by introducing mathematical and/or physical constraints, as for example smoothness of size distribution, positive number concentration (not trivial)

So let us reformulate the inverse problem

$$\cancel{g = A\,w \rightarrow w = A^{-1}\,g}$$

$\boxed{v(r) = w_j\,B_j(r)}$

Langrange multiplier, for example: 1E-3 … 1E+3

Error bound

$$e^2 \geq ||Aw - g||^2 + \gamma\Gamma$$

Constraint #1:
The solutions shall reproduce the optical input data as good as possible

Constraint #2:
The solutions shall be „smooth“;
the degree of smoothing is determined by the value of the Lagrange multiplier

Smoothing: $\gamma = 0$

$$e^2 \geq \| Aw - g \|^2 + \gamma\Gamma$$

Difference between input optical data and optical data that we obtain from our solutions on the microphysics

Suppression of oscillations of the size distribution, which can be expressed by means of a discrepancy parameter

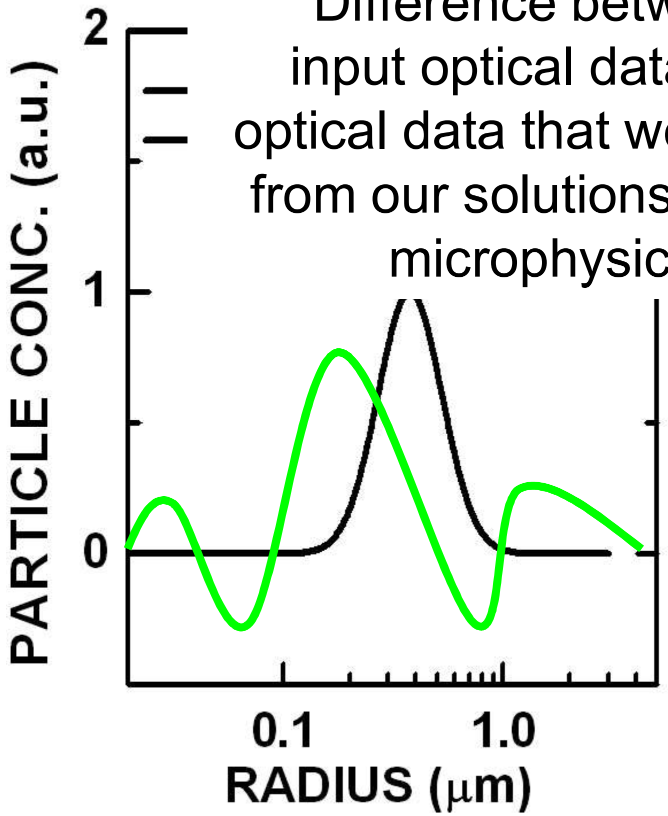

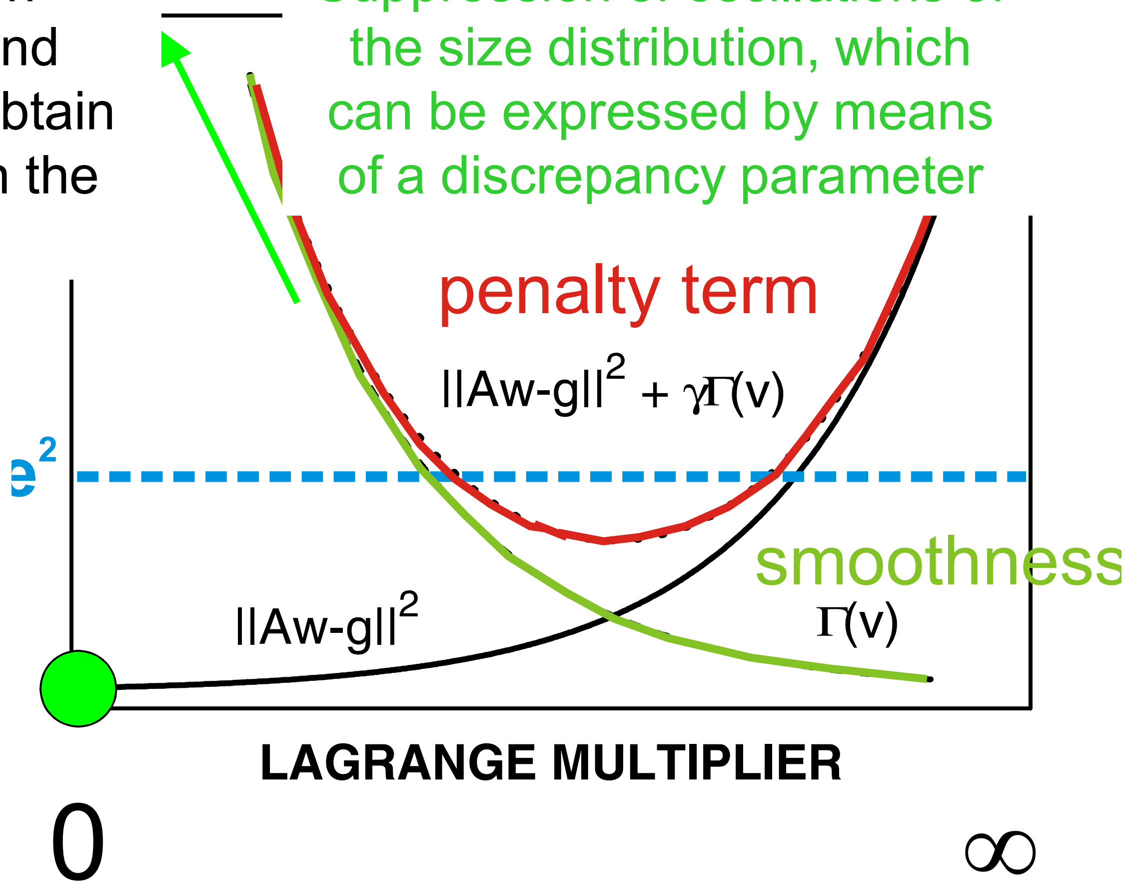

Smoothing: $\gamma \rightarrow \infty$

$$e^2 \geq \| Aw - g \|^2 + \gamma\Gamma$$

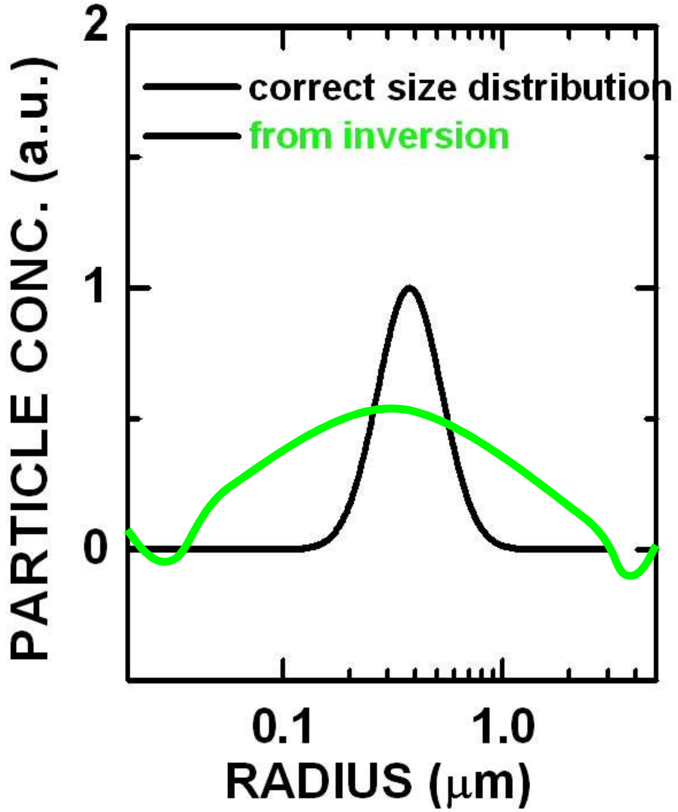

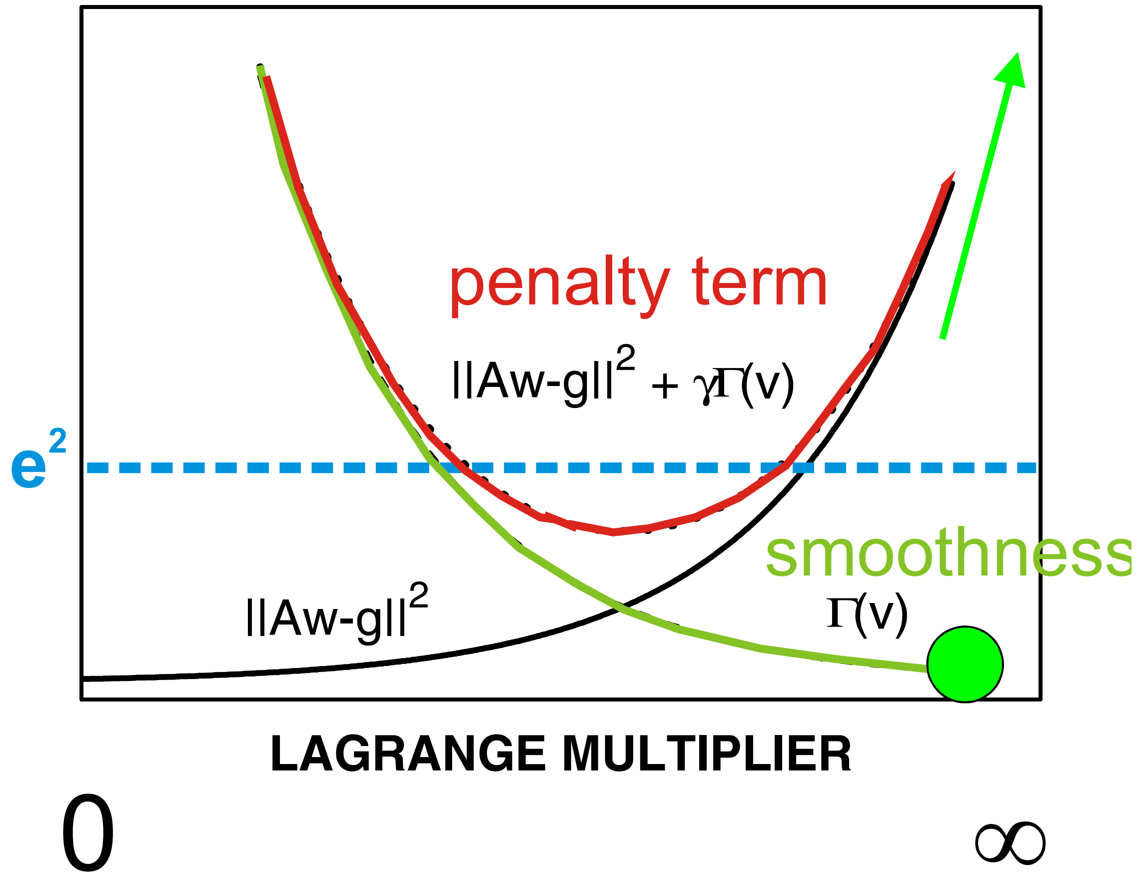

Smoothing: γ choosen in the „optimal“ way

Smoothing: γ choosen in the „optimal“ way

$$e^2 \geq \| Aw - g \|^2 + \gamma\Gamma$$

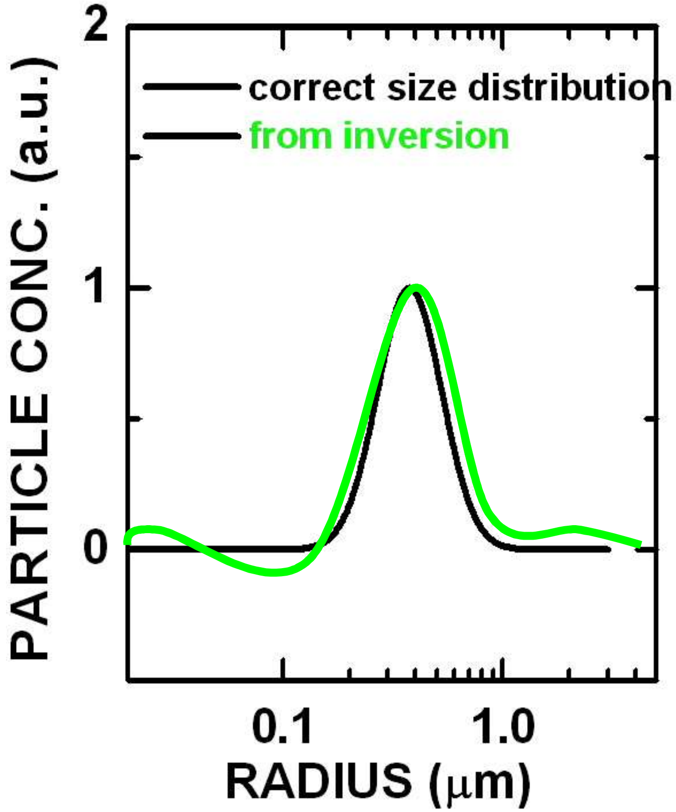

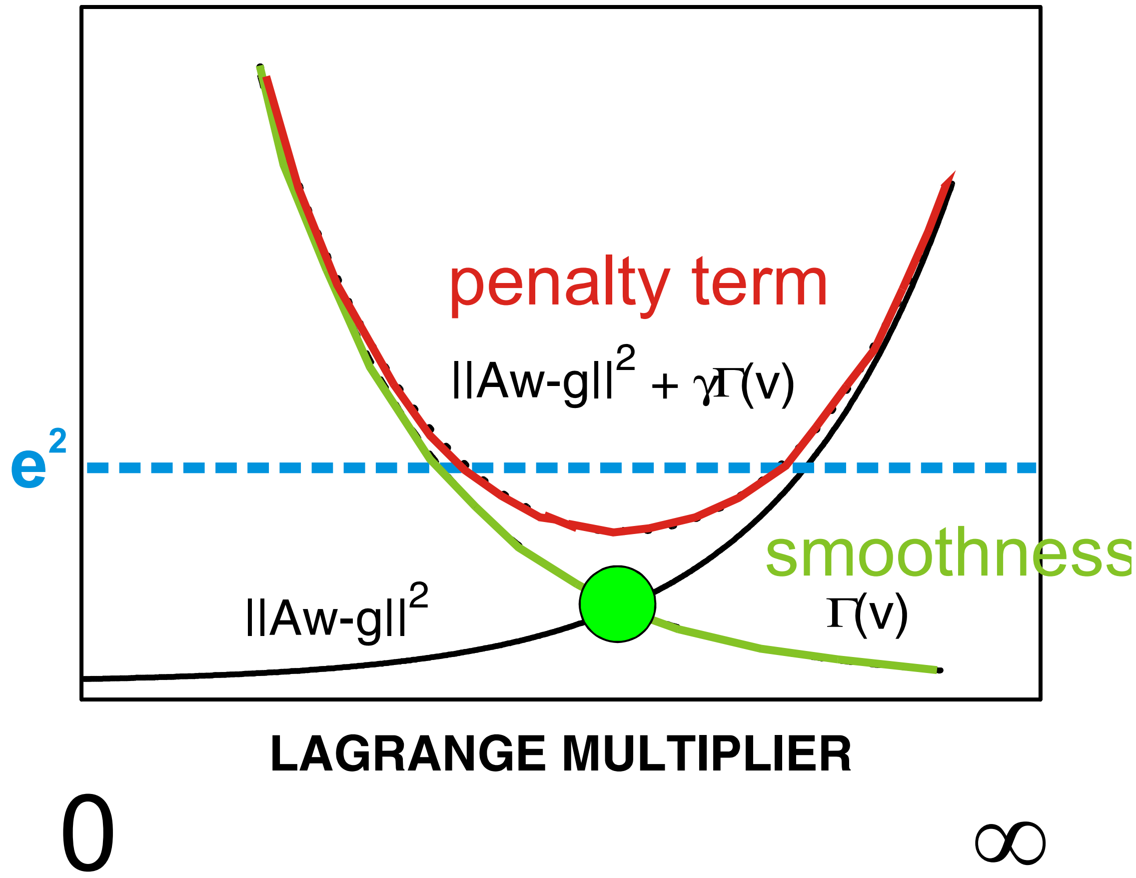

The mathematical solution of the weight factors follows after several mathematical operations

$$e^2 \geq ||Aw - g||^2 + \boxed{\gamma\Gamma}$$

$$\Downarrow$$

$$w = (A^T A + \boxed{\gamma H})^{-1} A^T g$$

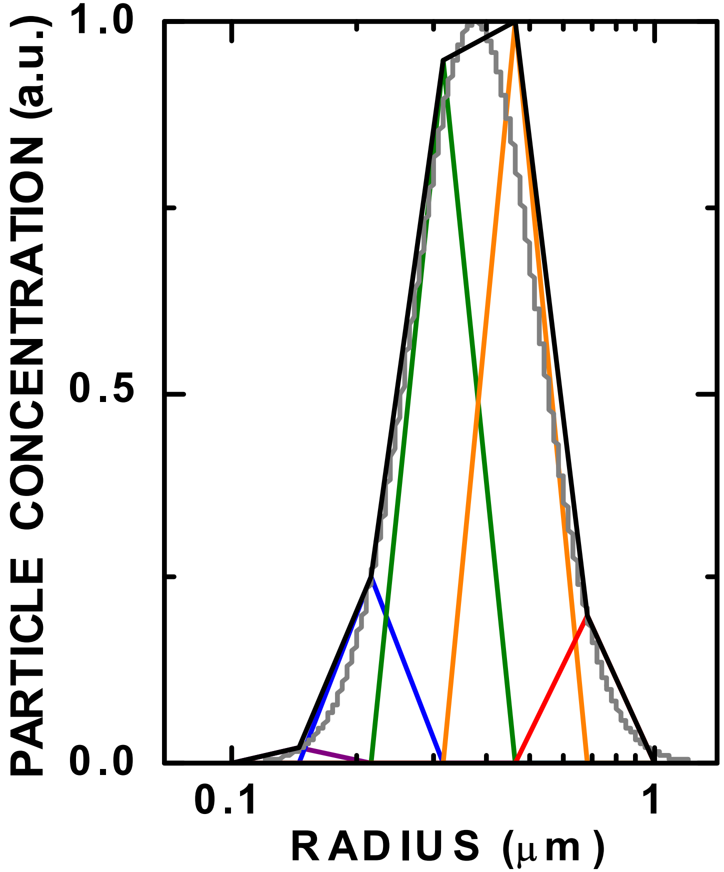

$$v(r) = w_j B_j(r)$$

(S. Twomey: Introduction to the mathematics of inversion in remote sensing and indirect measurements, Elsevier, Amsterdam, 1977)

The „smoothing“ term has a very simple mathematical form, e.g. second order smoothing

$$\boxed{\gamma \boldsymbol{\Gamma} \rightarrow \gamma \mathbf{H}}$$

- γ is a scalar
- H is a matrix

$$\mathbf{H} = \begin{bmatrix} 1 & -2 & 1 & 0 & 0 \\ -2 & 5 & -4 & 1 & 0 \\ 1 & -4 & 6 & -4 & 1 \\ 0 & 1 & -4 & 5 & -2 \\ 0 & 0 & 1 & -2 & 1 \end{bmatrix}$$

Number of rows:
Equals the number
of optical data

number of columns:
Equals the number of base functions

European Aerosol Research Lidar Network (EARLINET)

- Active since 2000, Funded by the European Commission
- Evolved from the German Lidar Network (1997 – 2000)
- Infrastructure Project:
  - Training, Teaching, Capacity Building
- Regular Measurements
  - Vertically Resolved Aerosol Climatology Over Europe

➢ Application of inversion algorithms increased

➢ Quality of the inversion products (microphysics) improved

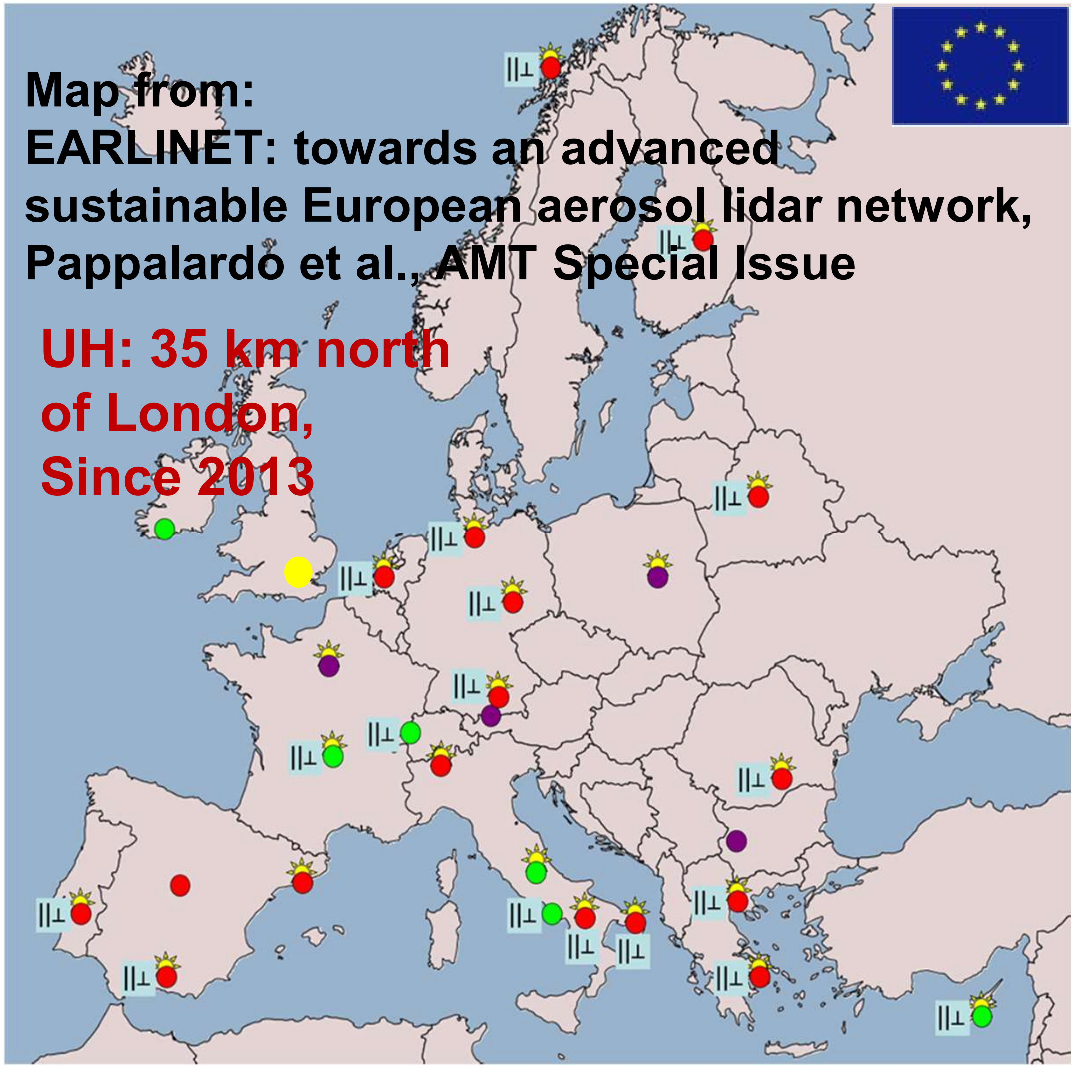

Multiwavelength 3+2 Raman Lidar Observations in Other Places, a Few Examples

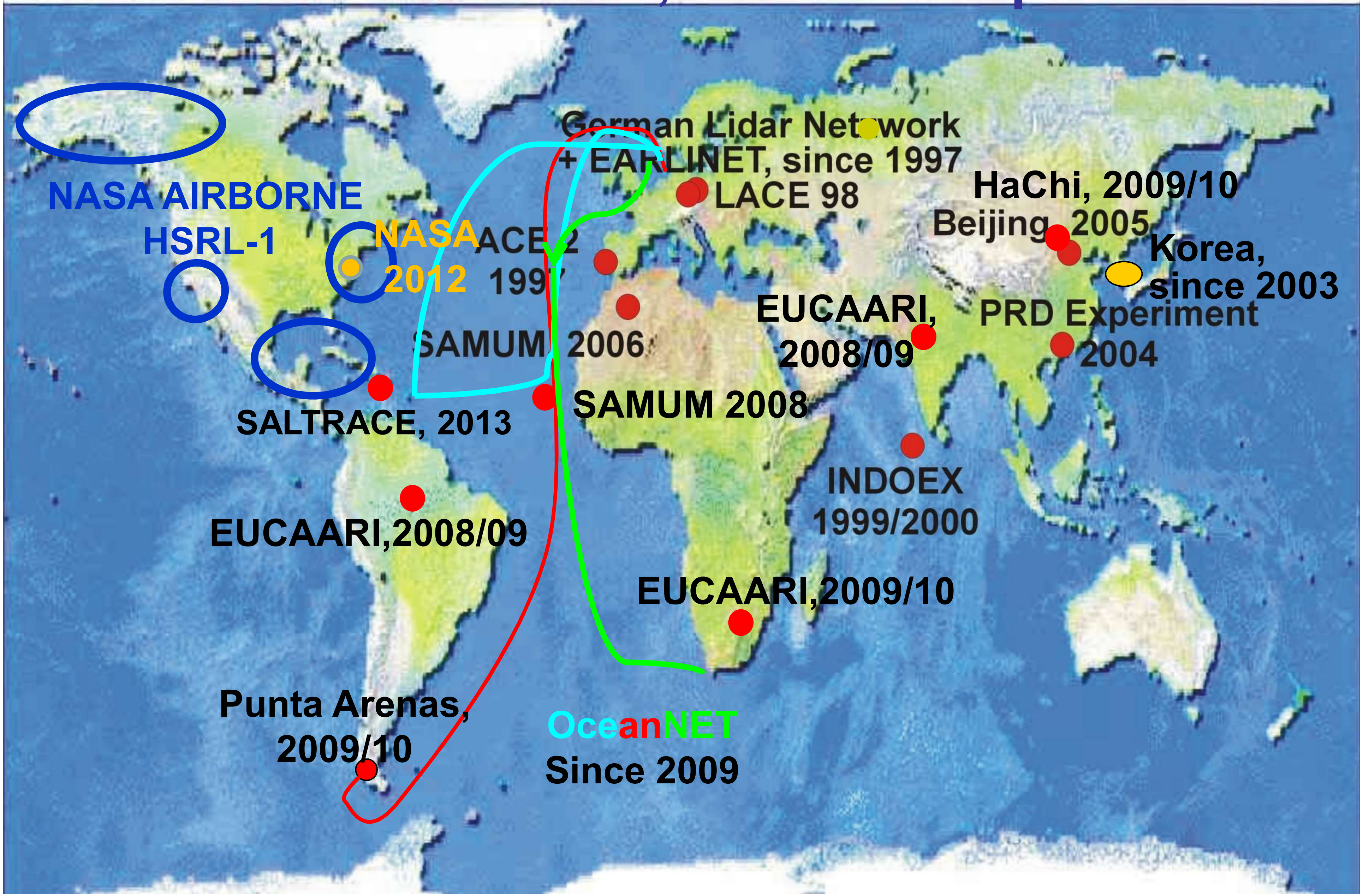

“Outpost” at the cross-road of East Asian pollution
Multi-wavelength Raman/Spectrometer Lidar in East Asia: MRS.LEA since 2009

Ideal place for feasibility studies with regard to what will be developed at UH

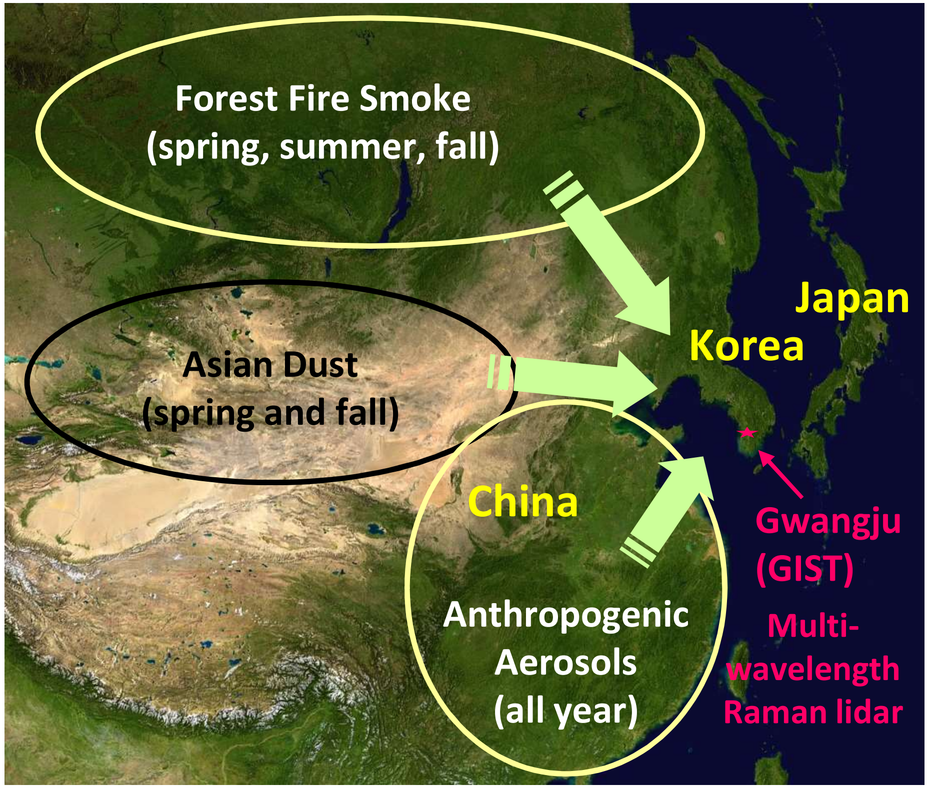

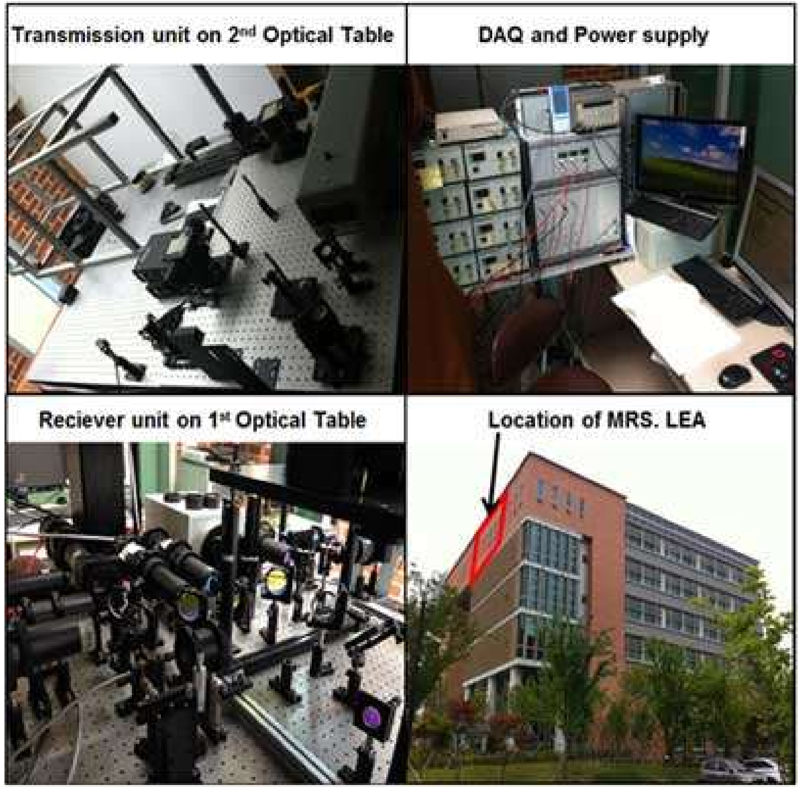

Comparison:
Forest-Fire Smoke – Anthropogenic Pollution

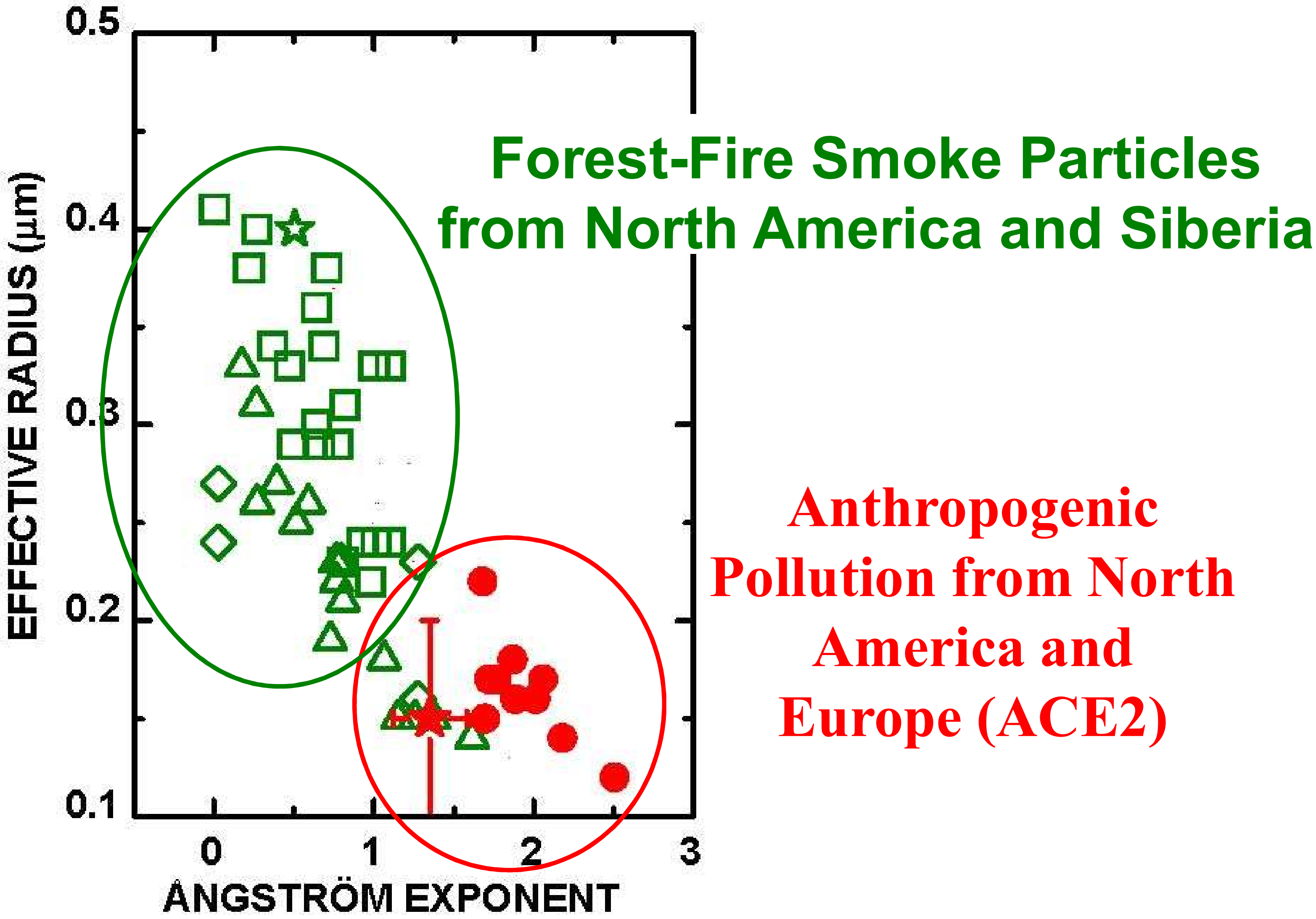

Change of Particle Properties With (Transport) Time

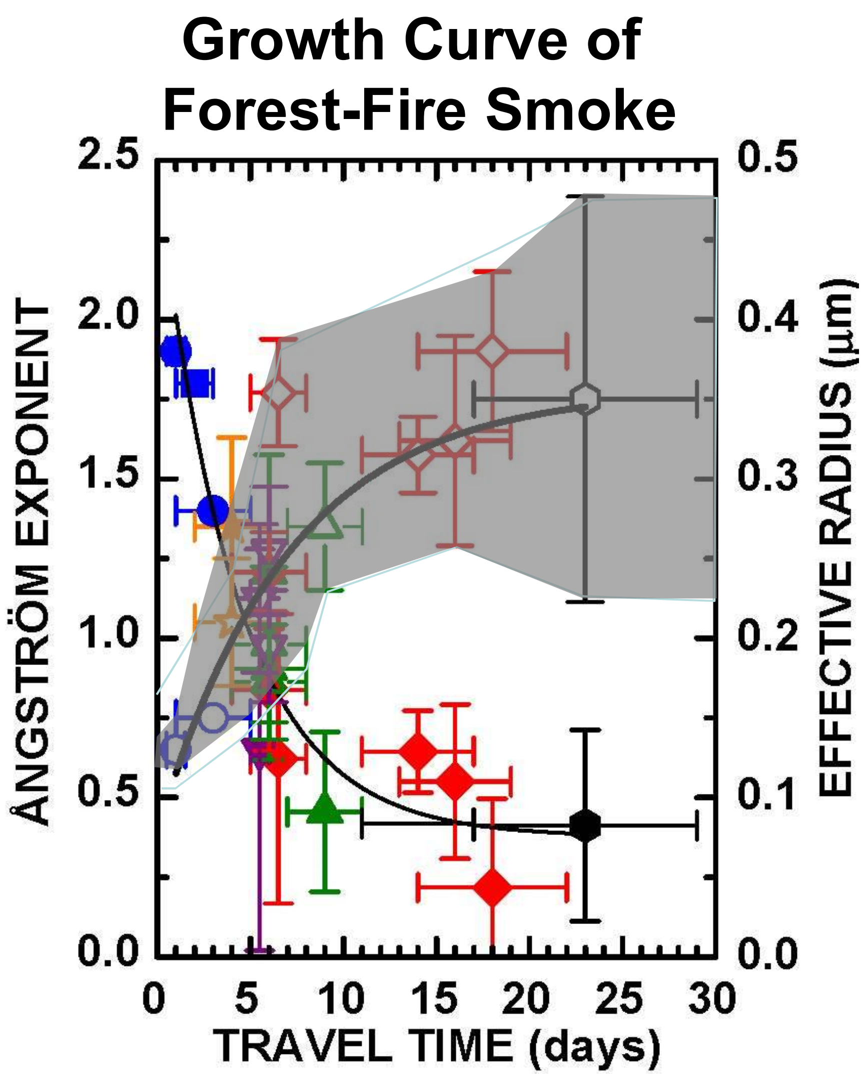

Dependence of particle size with transport time in various heights does have impact on:

- Light-absorption
- Cloud properties
- Radiation field

→ We lack in investigations of such effects

In-situ measurements (DLR aircraft) for the first 5 days
Fiebig et al., 2004

Müller et al., GRL 2007

Up to ~ 2006 comparably “few data” could be analyzed

Measurements at Leipzig and field campaign data, 100 – 150 data points

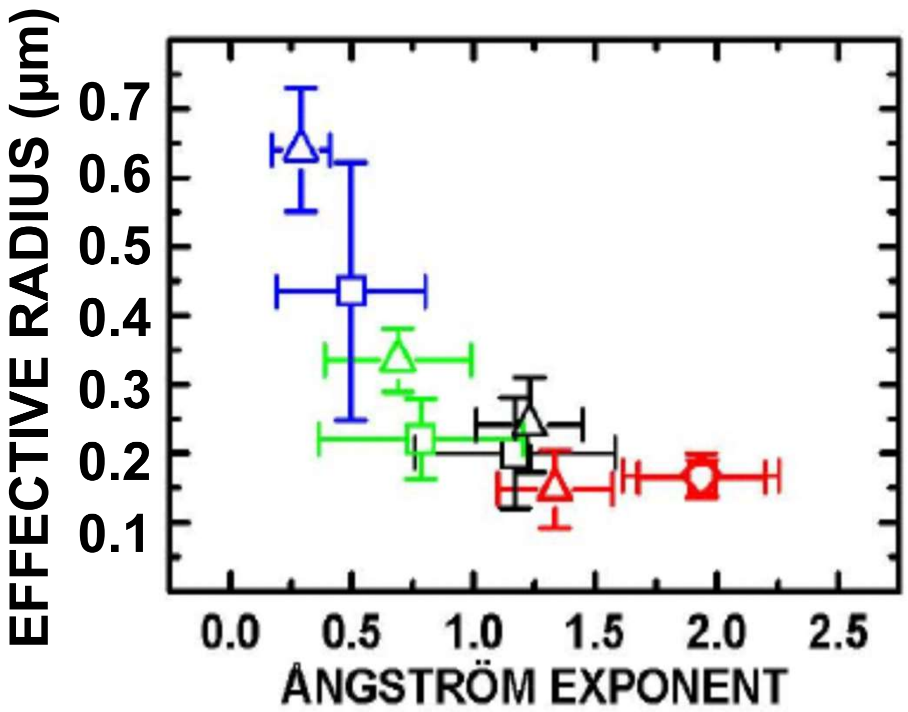

summary of results acquired between 2000 and 2006

Urban Haze from North America and inside Europe

Forest Fire Some From North America

South Asian Pollution

Marine at Coastal Station

Müller et al., JGR, 2002, 2003, 2004, 2005

Analysis of Data From Lidar in Different Locations of the World
A First Inventory on Aerosol Properties on the Vertical Scale collected since 1998 (incomplete list!!!)

Authors	Lidar site	Aerosol Type
Ansmann et al. (2000)	Maldives, Indian Ocean	South Asian haze, South Asian biomass burning smoke
Ansmann et al. (2009)	Cape Verde, Brazil	Saharan dust, West African biomass burning smoke
Böckmann et al. (2005)	Germany	Mixture of east European /Arctic haze
Eixmann et al. (2002)	Germany	Urban/industrial pollution from North America
Emgelmann et al. (2008)	Germany	European haze
Franke et al. (2003)	Maldives, Indian Ocean	South Asian haze, biomass burning smoke, maritime aerosol
Mattis et al. (2002)	Germany	Saharan dust
Mattis et al. (2003)	Germany	Canadian/Siberian forest fire smoke
Mattis et al.(2004)	Germany	European urban haze
Müller et al. (1998)	Germany	European urban haze
Müller et al. (2000a)	Maldives, Indian Ocean	South Asian haze. South biomass burning smoke
Müller et al. (2000b))	Portugal	European urban haze
Müller et al. (2001a)	Maldives, Indian Ocean	South Asian haze, South Asian biomass burning smoke
Müller et al. (2001b)	Germany	Canadian forest fire smoke
Müller et al. (2002)	Portugal	European urban haze
Müller et al. (2003a)	Maldives, Indian Ocean	South Asian haze, South Asian biomass burning smoke
Müller et al. (2003b)	Germany	Saharan dust
Müller et al. (2004)	Germany	Mixture of east European /Artic haze
Müller et al. (2005)	Germany	Canadian/Siberian forest fire smoke
Müller et al. (2007a)	Germany, Japan, South Korea and Spitsbergen	Forest fire smoke,transport,growth
Müller et al. (2007b)	Various sites on the globe	All aerosol types
Murayama et al. (2004)	Japan	Asian dust, Siberian smoke
Noh et al.(2007)	South Korea	Asian dust, East Asian haze
Noh et al.(2008)	South Korea	Asian dust, East Asian haze
Noh et al.(2009)	South Korea	Asian dust, East Asian haze, Siberian smoke
Tesche et al. (2009a)	Morocco	Saharan dust
Tesche et al. (2009b)	Cape Verde	Saharan dust, Africa biomass burning smoke
Wandinger et al. (2002)	Germany	European haze, Canadian forest fire smoke
Veselovskii et al. (2002)	Germany	European haze, Canadian forest fire smoke
Veselovski et al. (2004)	Germany	Southeast Asian biomass burning smoke

Next Step

Implementation of microphysics retrievals into unsupervised, automated software with real-time capacity

Motivation for This Step:
HSRL at NASA Langley Research Center

1st step: HSRL-1 development began ~2000
- backscatter at 355, 532, 1064nm; extinction at 532 nm
- measurements since 2006

2nd step: HSRL-2,
- based on HSRL-1 and in addition
- extinction at 355 nm and depolarization at 355, 532 and 1064 nm
- measurements since 2012

High Spectral Resolution Lidar (HSRL): basic principle

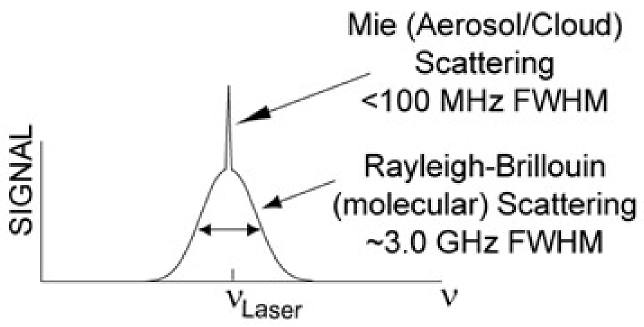

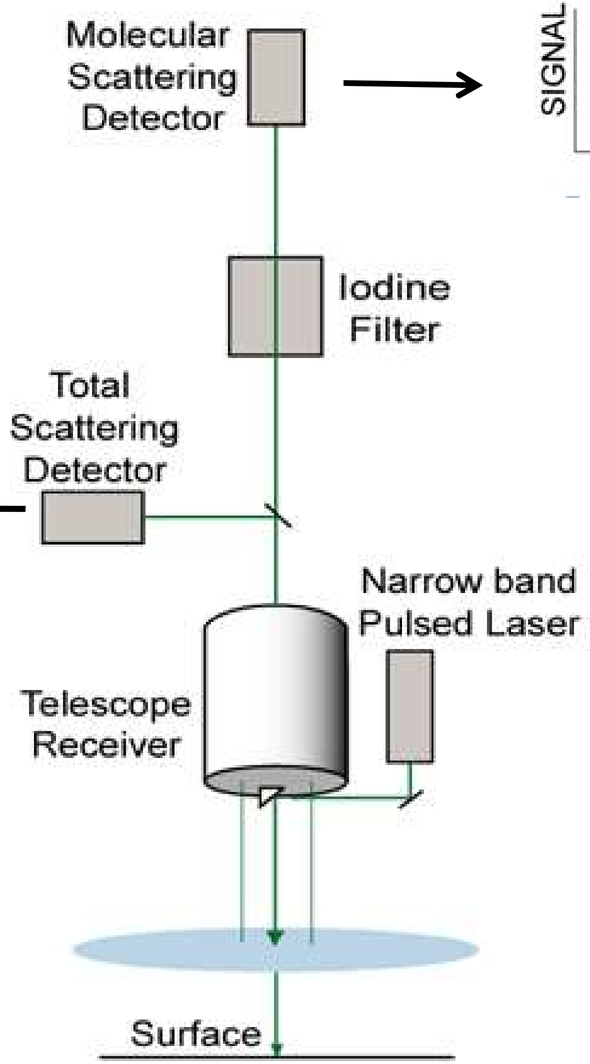

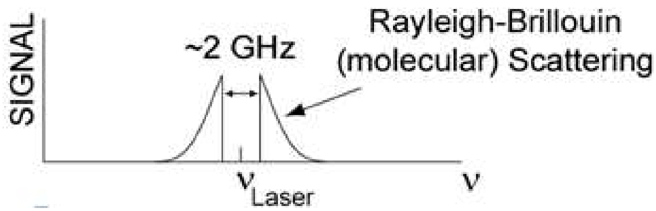

This channel measures the full spectrum of backscatter, including the particulate (Mie) backscatter and the broadened molecular backscatter

By tuning the laser to an iodine gas absorption line, this channel measures only the broadened molecular backscatter (the particulate backscatter is absorbed by the iodine gas).

The 2 channels provide 2 equations to solve for 2 unknowns:
- **aerosol extinction**
- **aerosol backscatter**

The "iodine technique" applies to 532 nm; interferometric approaches required for other wavelengths.

Airborne HSRL Aerosol Data Products

Note the variability in aerosol intensive parameters

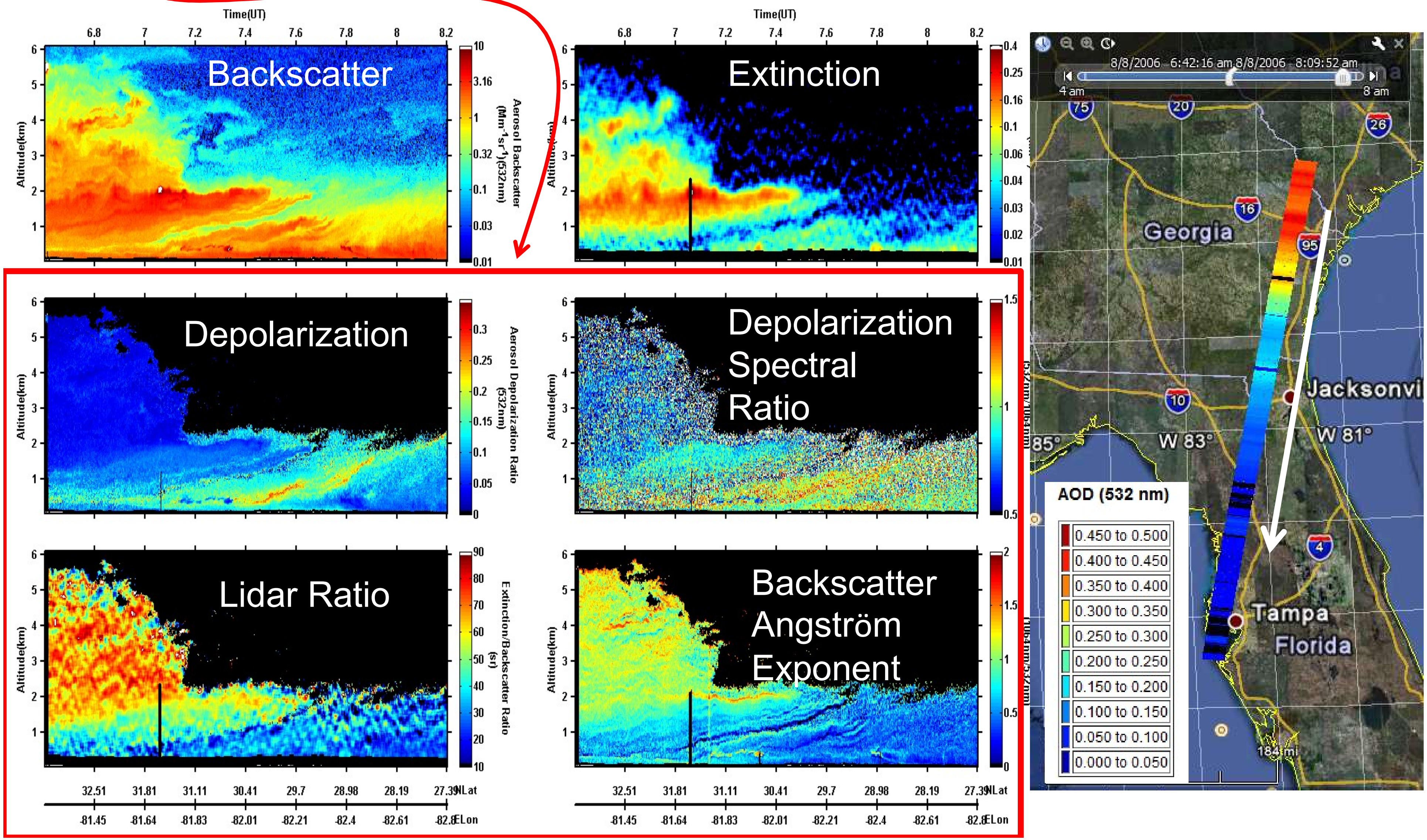

King Air B200 Field Campaigns with Langley High Spectral Resolution Lidar: HSRL-1 (3β+1α)

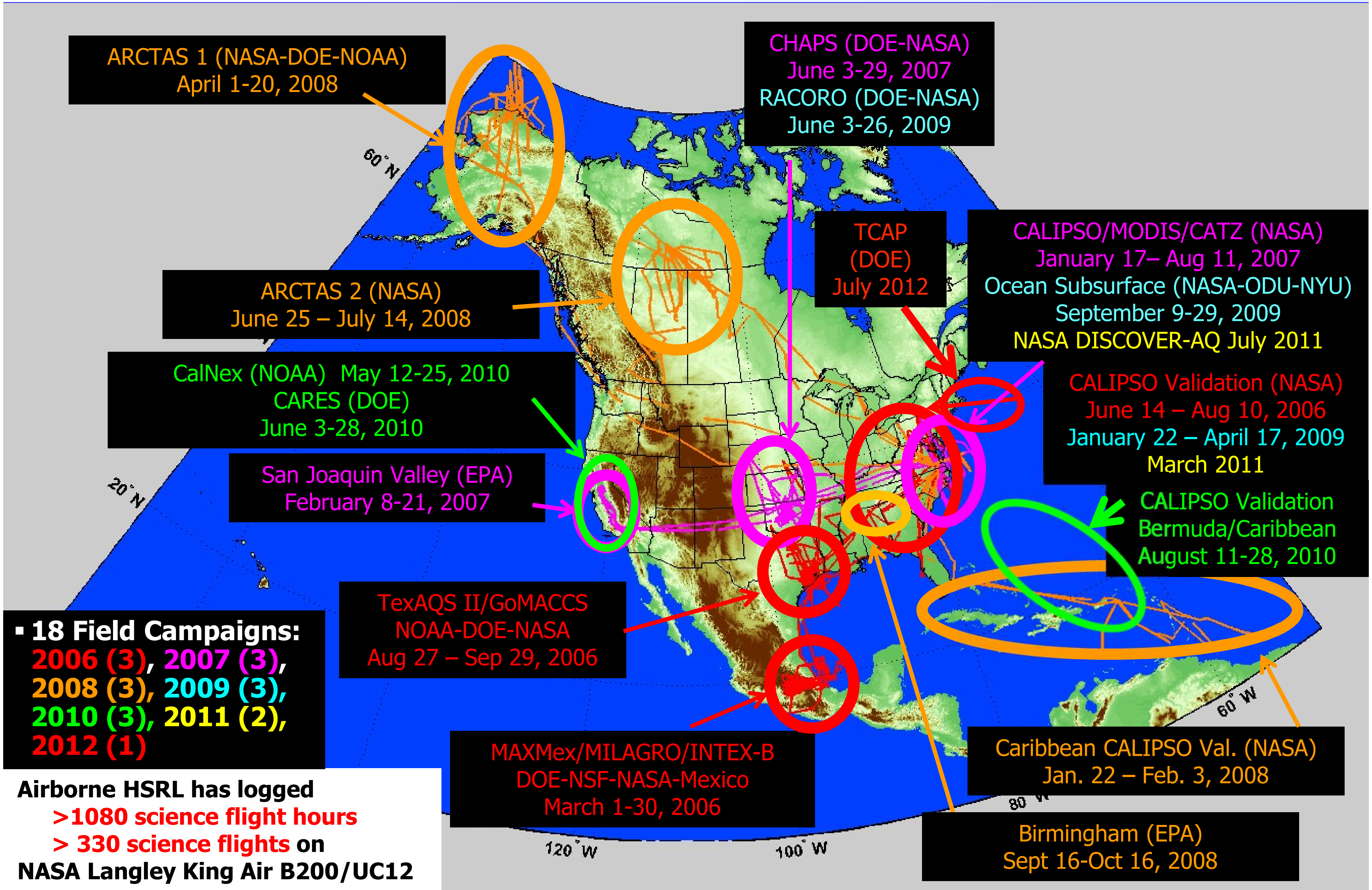

HSRL-1 data used to apportion aerosol optical depth by aerosol *type* and assess transport models

Fraction of AOT contributed by various aerosol types varies with location

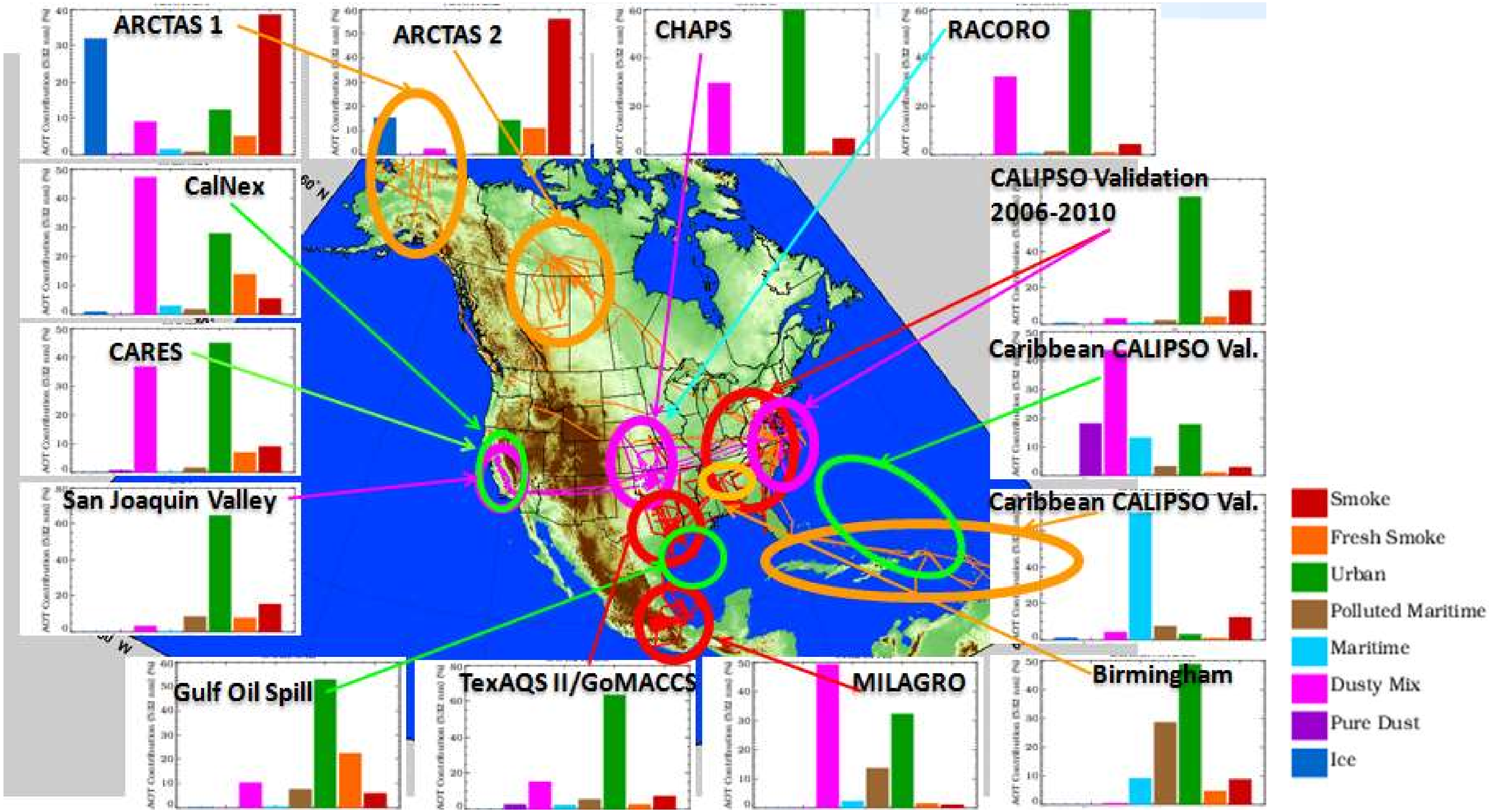

(Burton et al., 2011, AMT)

Aerosol Classification Using HSRL Measurements

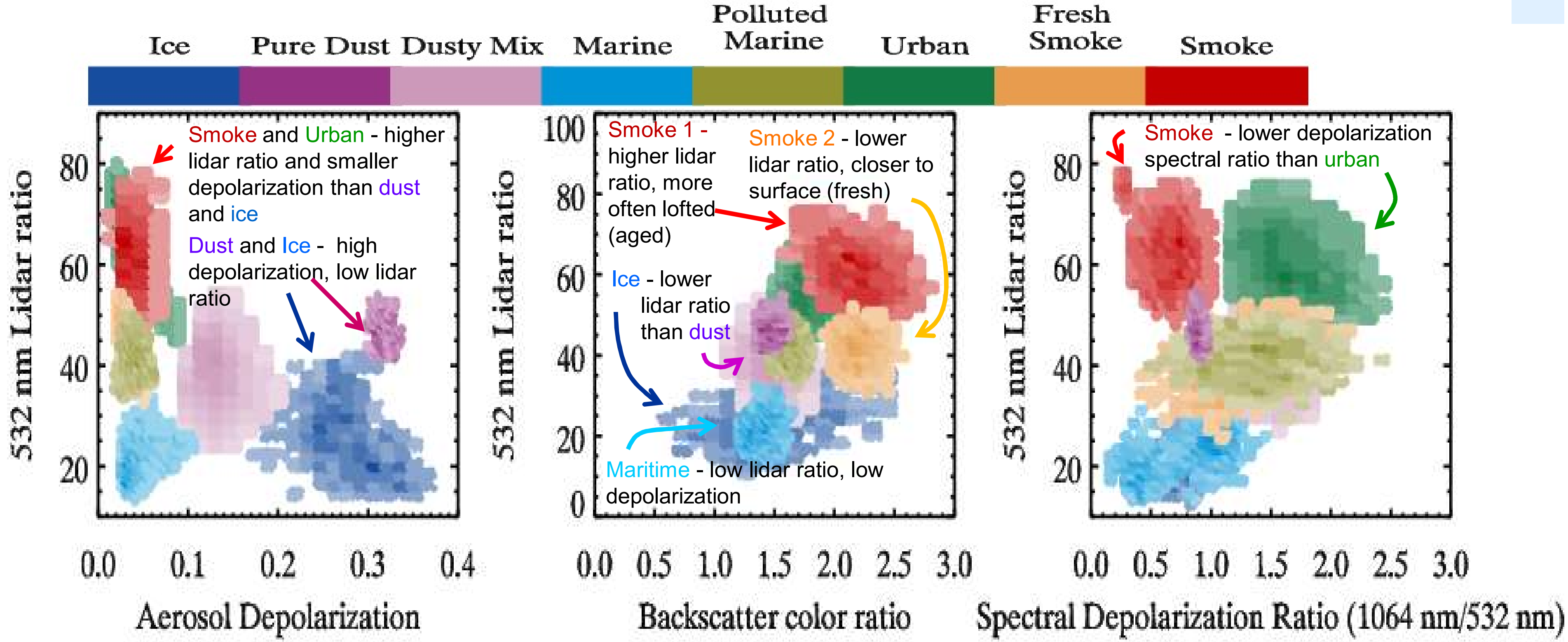

- Uses four aerosol intensive parameters to classify aerosols
- Employs a training set of known types
- Estimates the 4-D normal distributions of classes from labeled data
- Computes Mahalanobis distance to compute probability of each point belonging to each class
- HSRL data acquired from 2006-2012 are classified
- Technique described by Burton et al. (2012) (AMT)

King Air: ceiling ~ 9 km
ER-2: ceiling 30 km

Step toward spaceborne applications

- Objectives
  - Demonstrate technology
  - Validate lidar-only *3β+2α* aerosol microphysical retrievals

532-nm Signal from 17 July 2012 Flight off the Northeast Coast of the US (Boston Area)

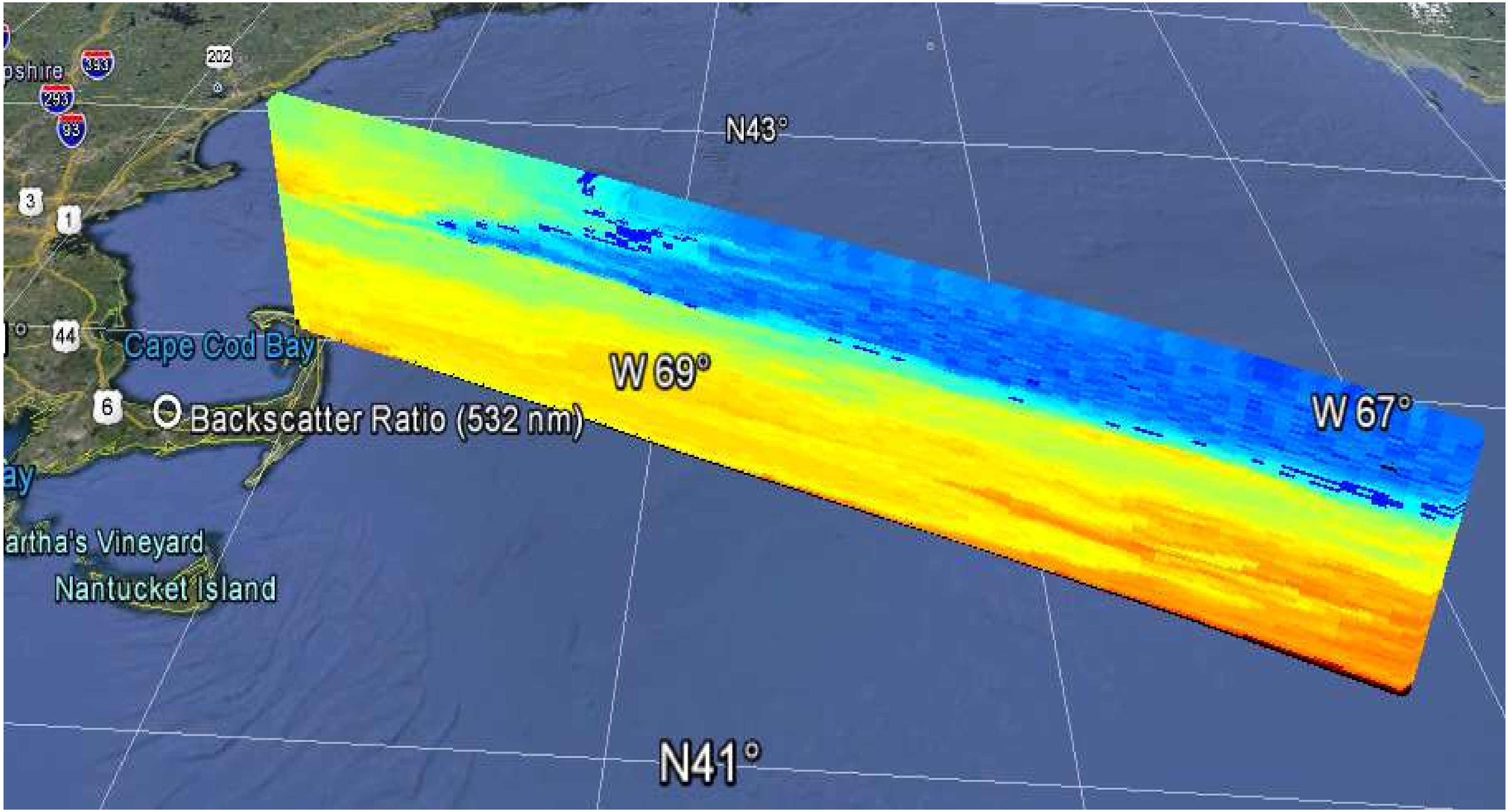

LaRC Airborne HSRL-2: First 3+2 HSRL

07/17/2012 TCAP flight on B200 aircraft

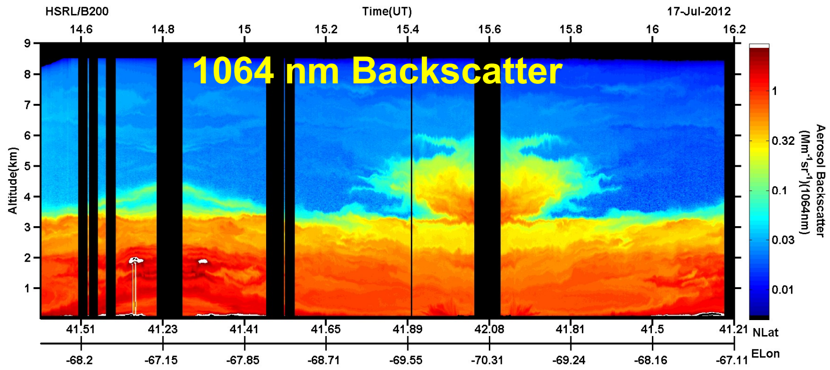

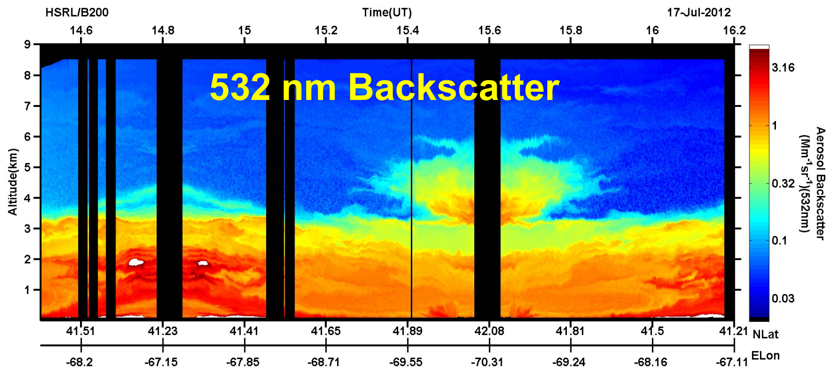

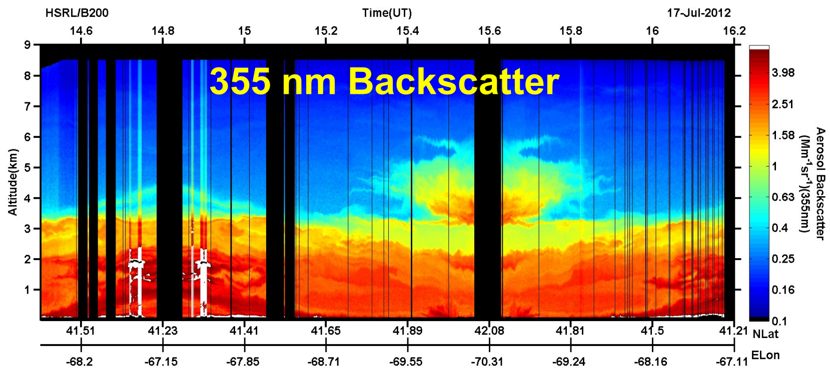

- High Spectral Resolution Lidar (HSRL) provides independent retrievals of aerosol extinction and backscatter
- HSRL-2 Capabilities
  - Backscatter at 355, 532, and 1064 nm
  - Extinction at 355 and 532 nm (HSRL)
  - Depolarization at 355, 532, 1064 nm

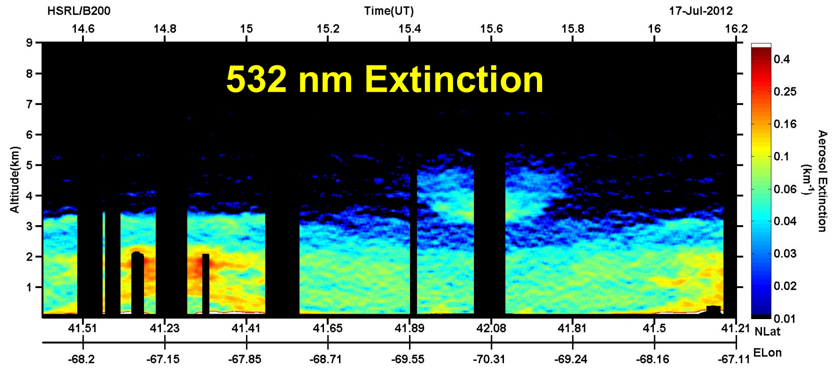

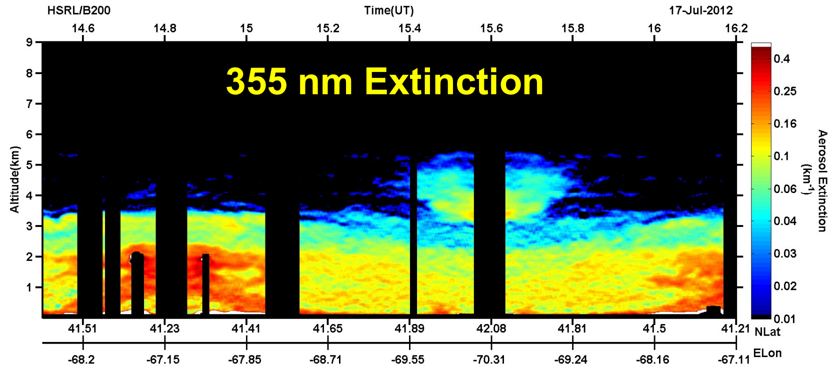

July 2012: proof of concept of automated inversion from optical to microphysical parameters with airborne NASA Langley HSRL-2 system

Airborne In –situ measurements

Inversion results from 3+2 system

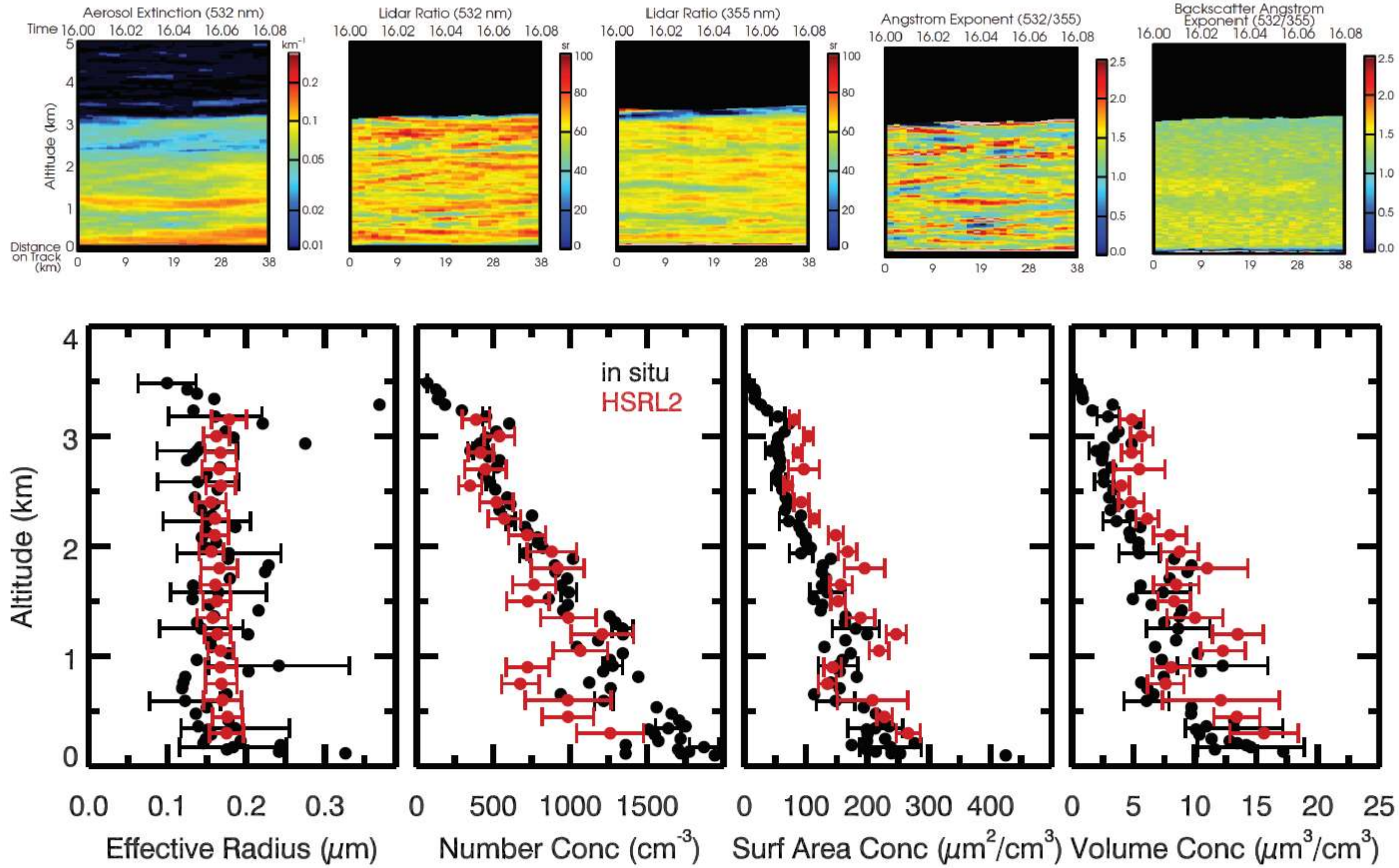

Figure 4. (Top) Curtain plots of an 5 min flight segment that was used for the data inversion. (Bottom) Microphysical parameters retrieved from the inversion method (red) and from the G-1 in situ measurements (black) on 17 July 2012. The measurement time was 16:00–16:05 UTC for the inversion results and 15:45–15:56 UTC for the in situ data. The lidar measurements were obtained 2 km from the approximate G-1 spiral center. The inversion results represent height intervals of 150 m. The in situ data were taken with considerably higher spatial resolution. Error bars of the individual in situ data points are composed of two types, counting and sizing. The error bars denote 1 standard deviation.

Müller et al., AMT, 7, 3487 – 3496, 2014

TCAP Field Campaign: Profiles, Curtain Plots

- **Each curtain plot:**
  - **73 lidar profiles**
  - **ca. 3 hours flighttime**
  - **2035 sets of 3β + 2α data**

- **36 hours processing time in 2012**
- **about 1 hour processing time in 2015**

Angström Exponent: 1 – 1.5

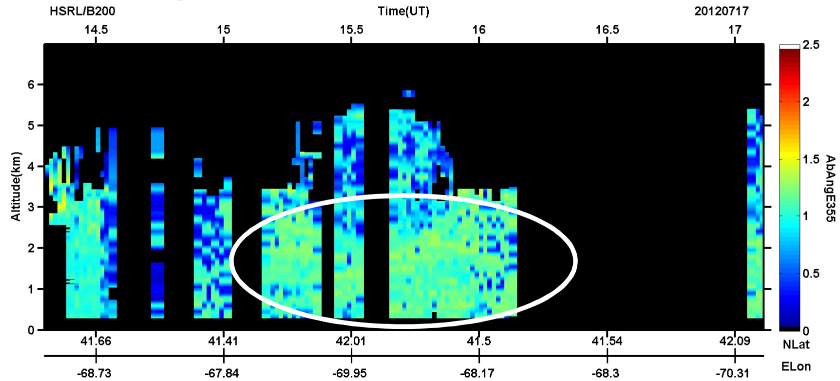

Effective Radius: 0.15 – 0.25 µm

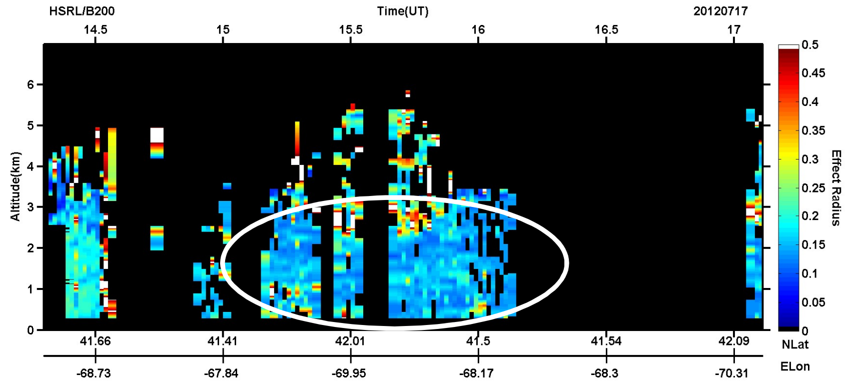

TCAP Field Campaign: Fresh Smoke?

Imaginary Part

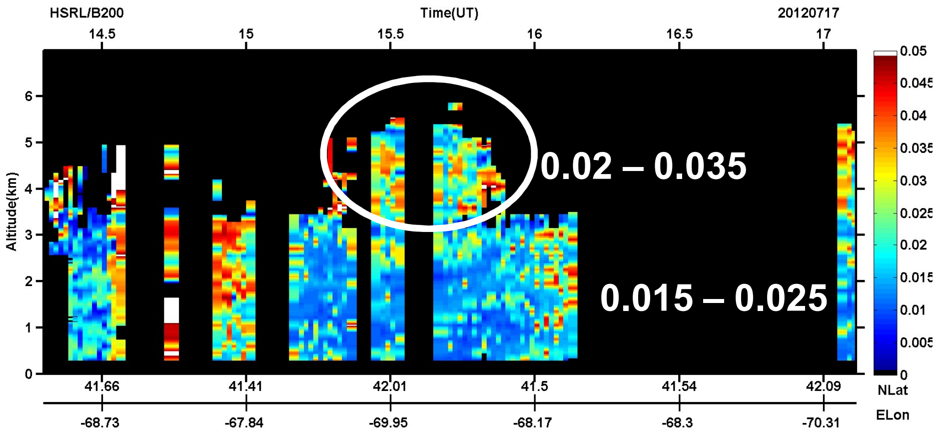

Single-Scatt Albedo @532nm

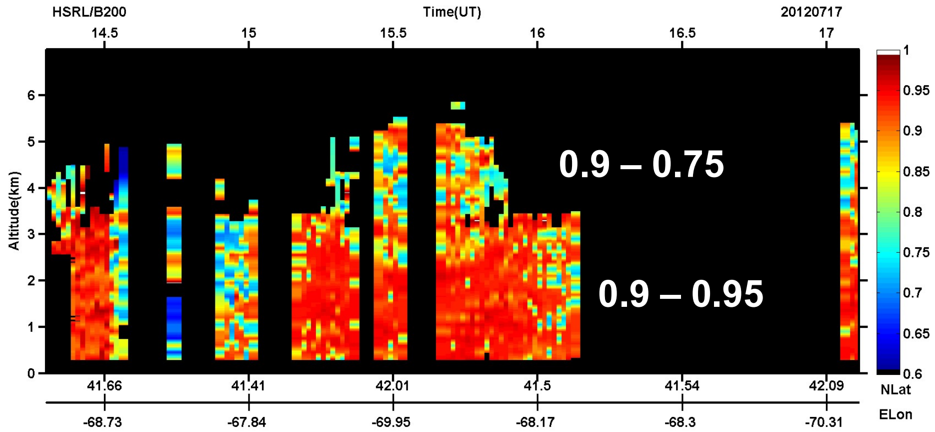

Absorption Coeff.@532nm

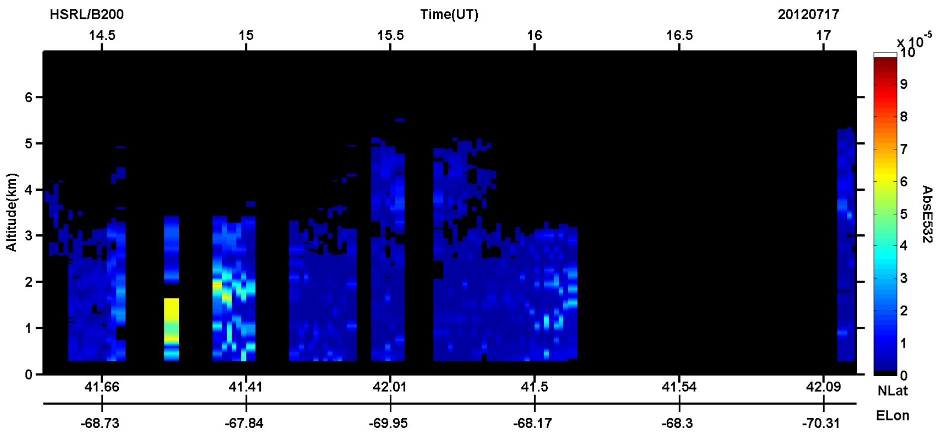

Absorption Angström Exp.

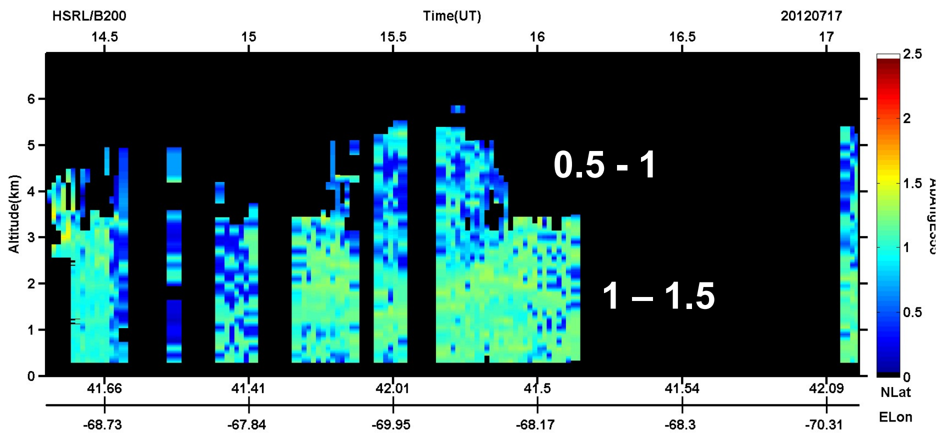

Aerosol-Cloud-Ecosystems Mission (ACE)

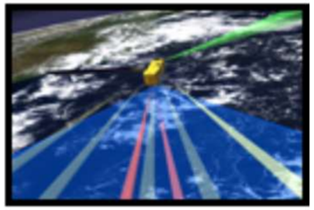

Launch: ~2025 (2030)???

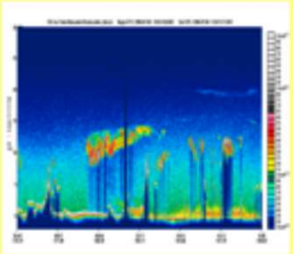

Cloud and aerosol height

Organic material in surface ocean layers

Aerosol and cloud types and properties

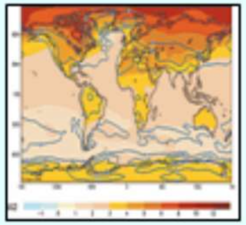

Improved climate models

Local climate change prediction

Ocean productivity

Ocean health

Air quality models and forecasts

Instruments: lidar, polarimeter, radar, ocean-color spectro-radiometer

Optical and microphysical aerosol parameters

Extensive optical particle parameters

Particle volume backscatter coefficient: 355, 532, and 1064 nm;
Particle volume extinction coefficient: 355 and 532 nm;
Raman quartz backscatter coefficient at 360 and 546 nm;

Intensive optical particle parameters

Linear particle polarization ratio: 532 nm;
Particle lidar ratio: 355 and 532 nm;
Extinction-related Ångström exponent: 355/532-nm wavelength pair;
Backscatter-related Ångström exponent: 355/532-nm and 532/1064-nm wavelength pairs;
Raman-quartz backscatter-related Ångström exponent: 360/546-nm wavelength pair

Microphysical particle parameters (from inversion of extensive optical properties)

Real and imaginary part of the complex refractive index;
number, volume and surface-area concentration; particle volume size distribution; particle effective radius;

„High-end“ particle parameters

Single-scattering albedo
Phase function